ADVANCED HYBRID PARTICULATE COLLECTOR – PHASE III

Quarterly Technical Progress Report
for the period July 1, 2000, through September 30, 2000

Prepared for:

AAD Document Control
U.S. Department of Energy
National Energy Technology Laboratory
PO Box 10940, MS 921-143
Pittsburgh, PA 15236-0940

DOE Contract No. DE-FC26-99FT40719
Performance Monitor: William Aljoe

Prepared by:

Stanley J. Miller
Ye Zhuang
Michael E. Collings
Michelle R. Olderbak

Energy & Environmental Research Center
University of North Dakota
PO Box 9018
Grand Forks, ND 58202-9018

Richard Gebert
Dwight Davis

W.L. Gore & Associates, Inc.
101 Lewisville Road
PO Box 1100
Elkton, MD 21922-1100

October 2000

EERC DISCLAIMER

LEGAL NOTICE This research report was prepared by the Energy & Environmental Research Center (EERC), an agency of the University of North Dakota, as an account of work sponsored by National Energy Technology Laboratory. Because of the research nature of the work performed, neither the EERC nor any of its employees makes any warranty, express or implied, or assumes any legal liability or responsibility for the accuracy, completeness, or usefulness of any information, apparatus, product, or process disclosed, or represents that its use would not infringe privately owned rights. Reference herein to any specific commercial product, process, or service by trade name, trademark, manufacturer, or otherwise does not necessarily constitute or imply its endorsement or recommendation by the EERC.

DISCLAIMER

This report was prepared as an account of work sponsored by an agency of the United States Government. Neither the United States Government, nor any agency thereof, nor any of their employees makes any warranty, express or implied, or assumes any legal liability or responsibility for the accuracy, completeness, or usefulness of any information, apparatus, product, or process disclosed or represents that its use would not infringe privately owned rights. Reference herein to any specific commercial product, process, or service by trade name, trademark, manufacturer, or otherwise does not necessarily constitute or imply its endorsement, recommendation, or favoring by the United States Government or any agency thereof. The views and opinions of authors expressed herein do not necessarily state or reflect those of the United States Government or any agency thereof.

This report is available to the public from the National Technical Information Service, U.S. Department of Commerce, 5285 Port Royal Road, Springfield, VA 22161; phone orders accepted at (703) 487-4650.

ACKNOWLEDGMENT

This report was prepared with the support of the U.S. Department of Energy (DOE) National Energy Technology Laboratory Contract No. DE-FC26-99FT40719. However, any opinions, findings, conclusions, or recommendations expressed herein are those of the authors(s) and do not necessarily reflect the views of DOE.

TABLE OF CONTENTS

LIST OF FIGURES ii

LIST OF TABLES iv

ABSTRACT v

EXECUTIVE SUMMARY vi

1.0 INTRODUCTION 1

2.0 PHASE III OBJECTIVES AND PLANNED WORK 1

3.0 FLOW THEORY AND PERFORMANCE EVALUATION CRITERIA 1

4.0 AHPC RESULTS FROM BIG STONE 4
- 4.1 Analysis of Bag-Cleaning Interval 4
- 4.2 AHPC Model Modification 11

5.0 FILTER BAG EVALUATION 15
- 5.1 Visual Analysis 16
- 5.2 Media Analysis 18
- 5.3 Dimensional Analysis 18
- 5.4 Air Permeability Analysis 19
- 5.5 Mechanical Strength Analysis 20
- 5.6 Summary of Bag Evaluation 20

6.0 COLD-FLOW TESTS AT THE EERC 20
- 6.1 Effect of Electrodes on V-I Characteristics and Current to Bags 22
- 6.2 EERC Electrode Tests 25
- 6.3 EX Electrode Tests 25
- 6.4 EN Electrode Tests 28
- 6.5 Summary of the Cold-Flow Tests 32

7.0 PLANS FOR NEXT QUARTER 33

LIST OF FIGURES

1 Daily average pressure drop for June 28–July 5 5

2 Residual drag for June 28–July 5 5

3 Bag-cleaning interval for June 28–July 5 6

4 K_2C_i as a function of bag-cleaning interval for June 28–July 5 6

5 Pressure drop for July 7 7

6 Bag-cleaning interval for July 7 7

7 K_2C_i for July 7 8

8 K_2C_i versus difference in pressure drop before and after bag cleaning for July 7 9

9 Bag-cleaning interval versus K_2C_i for July 7 9

10 A/C ratio for July 9 10

11 Pressure drop for July 9 10

12 Bag-cleaning interval for July 9 11

13 K_2C_i versus bag-cleaning interval for July 9 12

14 K_2C_i versus velocity 14

15 Comparison of predicted time interval with experimental results 15

16 Row 2 Bag 2 after brushing 17

17 Effect of electrode on V-I characteristics 23

18 Effect of electrode on V-I characteristics 23

19 Effect of electrode on current to bags 24

20 Effect of electrode on current to bags 24

Continued . . .

LIST OF FIGURES (Continued)

21 Effect of spacing ratio on bag current 26

22 Effect of plate spacing on bag current 26

23 Effect of grid on bag current 27

24 Effect of ratio on current to the bags 27

25 Effect of bag type on current to the bags 29

26 Effect of bag type on current to the bags 29

27 Effect of grounded grid on current to the bags 30

28 Effect of ratio on current to the bags 30

29 Effect of ratio on current to the bags 31

30 Effect of bag type on current to the bags 31

31 Effect of bag type on current to the bags in the presence of a grounded grid 32

LIST OF TABLES

1 Experimental Results 13

2 Experimental Results and the Predicted Time Interval under Normal AHPC Performance 14

3 Filter Media Permeability as Measured in Lab 20

4 Electrode Type and Discharge Points 21

ADVANCED HYBRID PARTICULATE COLLECTOR – PHASE III

ABSTRACT

A new concept in particulate control, called an advanced hybrid particulate collector (AHPC), is being developed under funding from the U.S. Department of Energy. The AHPC combines the best features of electrostatic precipitators (ESPs) and baghouses in a unique configuration. The AHPC concept consists of a combination of fabric filtration and electrostatic precipitation in the same housing, providing major synergism between the two collection methods, both in the particulate collection step and in the transfer of dust to the hopper. The AHPC provides ultrahigh collection efficiency, overcoming the problem of excessive fine-particle emission with conventional ESPs, and it solves the problem of reentrainment and re-collection of dust in conventional baghouses. In Phase II, a 2.5-MW-scale AHPC was designed, constructed, installed, and tested at the Big Stone power station. For Phase III, further testing of an improved version of the 2.5-MW-scale AHPC at the Big Stone power station is being conducted to facilitate commercialization of the AHPC technology.

ADVANCED HYBRID PARTICULATE COLLECTOR – PHASE III

EXECUTIVE SUMMARY

A new concept in particulate control, called an advanced hybrid particulate collector (AHPC), is being developed at the Energy & Environmental Research Center (EERC) with U.S. Department of Energy (DOE) funding. In addition to DOE and the EERC, the project team includes W.L. Gore & Associates, Inc.; Allied Environmental Technologies, Inc.; and the Big Stone power station. The AHPC combines the best features of electrostatic precipitators (ESPs) and baghouses in a unique approach to develop a compact but highly efficient system. Filtration and electrostatics are employed in the same housing, providing major synergism between the two collection methods, both in the particulate collection step and in the transfer of dust to the hopper. The AHPC provides ultrahigh collection efficiency, overcoming the problem of excessive fine-particle emissions with conventional ESPs, and solves the problem of reentrainment and re-collection of dust in conventional baghouses.

The objective of the project is to develop a highly reliable AHPC that can provide >99.99% particulate collection efficiency for particle sizes from 0.01 to 50 µm, is applicable for use with all U.S. coals, and is less costly than existing technologies.

Phase I of the development effort consisted of design, construction, and testing of a 200-acfm (5.7-m^3/min) working AHPC model. Coal-fired test results with a pilot-scale system showed that the concept worked well, achieving greater than 99.99% collection efficiency for fine particles at high filtration velocities.

Since all of the developmental goals of Phase I were met, the approach was scaled up in Phase II to a size of 9000 acfm (255 m^3/min equivalent in size to 2.5 MW) and was installed on a slipstream at the Big Stone power station.

For Phase II, the AHPC at Big Stone power station was operated continuously from late July 1999 until mid-December 1999, except for a 3-week down period in September corresponding to an annual plant outage. The Phase II results were highly successful in that ultrahigh particle collection efficiency was achieved, pressure drop was well controlled, and system operability was excellent.

For Phase III, the developmental objective is to obtain the necessary engineering data to facilitate scaleup of the AHPC to the full-scale demonstration size for near-term commercialization of this technology. The approach to meet the Phase III objectives is continued testing of the 9000-acfm (255-m^3/min) field demonstration AHPC at the Big Stone power station. The test plan includes seven 1-month tests: six to address a specific primary variable and one to serve as a contingency test. In addition to the testing at the Big Stone plant, the test plan also includes supporting laboratory tests and approximately 2 weeks of further testing with the 200-acfm (5.7-m^3/min) AHPC at the EERC. The field AHPC unit was successfully started up in April 2000 and was operated for a period of about 3 months through July 2000. Initial results,

reported in the April to June Quarterly Report, showed that the AHPC with the modified configuration exceeded the performance goals of a 10-min bag-cleaning interval at an air-to-cloth (A/C) ratio of 12 ft/min (3.7 m/min) and 8-in. W.C. (2.0-kPa) pressure drop. Excellent performance was achieved in spite of having to deal with a fine-particle size, high-resistivity ash. Results showed that the bag-cleaning interval is quite sensitive to A/C ratio and can be significantly increased by a small reduction in A/C ratio for a constant pulse-cleaning set point. Alternatively, the average pressure drop can be significantly reduced by a small reduction in A/C ratio at a constant bag-cleaning interval.

During July, further tests at Big Stone were completed to help establish the relationships among pressure drop, bag-cleaning interval, and A/C ratio. Bags were also removed from the Big Stone AHPC for inspection in June and July. Additional testing with the 200-acfm (5.7-m^3/min) AHPC at EERC was also completed in August and September to evaluate electrode design and geometric spacing.

ADVANCED HYBRID PARTICULATE COLLECTOR – PHASE III

1.0 INTRODUCTION

This project was awarded under the U.S. Department of Energy (DOE) Program Solicitation DE-PA26-99FT40251 and specifically addresses Technical Topical Area 3 – Primary PM Emissions Control. Phase III is a logical continuation of the development toward full-scale commercialization of the advanced hybrid particulate collector (AHPC).

2.0 PHASE III OBJECTIVES AND PLANNED WORK

The objective of the project is to develop a highly reliable AHPC that can provide >99.99% particulate collection efficiency for all particle sizes from 0.01 to 50 µm, is applicable for use with all U.S. coals, and is less costly than existing technologies. This goal has remained unchanged since the concept was originally proposed in 1994. The approach objective with the AHPC is to utilize filtration and electrostatic mechanisms in a unique manner that is superior to conventional fabric filters and electrostatic precipitators (ESPs). The developmental objective for Phase III is to obtain the necessary engineering data to facilitate scaleup of the AHPC to the full-scale demonstration size for near-term commercialization of this technology.

The Phase III planned work includes seven 1-month tests at Big Stone as well as supporting laboratory tests and approximately 2 weeks of further testing with the 200-acfm (5.7-m^3/min) AHPC at the Energy & Environmental Research Center (EERC).

The field AHPC unit was successfully started up in April 2000 and was operated for a period of about 3 months through July 2000. Additional testing with the 200-acfm (5.7-m^3/min) AHPC at the EERC was also completed in August and September to evaluate electrode design and geometric spacing.

3.0 FLOW THEORY AND PERFORMANCE EVALUATION CRITERIA

For viscous flow, pressure drop across a fabric filter is dependent on three components:

$$dP = K_f V + K_2 W_R V + K_2 C_i V^2 t / 7000 \qquad \text{[Eq. 1]}$$

where:

- dP = differential pressure across baghouse tube sheet (in. W.C.) (kPa)
- K_f = fabric resistance coefficient (in. W.C.-min/ft) (kPa-min/m)
- V = face velocity or A/C ratio (ft/min) (m/min)
- K_2 = specific dust cake resistance coefficient (in. W.C.-ft-min/lb) (kPa-m-min/kg)
- W_R = residual dust cake weight (lb/ft^2) (kg/m^2)
- C_i = inlet dust loading (grains/acf) (g/m^3)

t = filtration time between bag cleaning (min)

The first term in Eq. 1 accounts for the pressure drop across the fabric. For conventional fabrics, the pore size is quite large, and the corresponding fabric permeability is high, so the pressure drop across the fabric alone is negligible. To achieve better collection efficiency, the pore size can be significantly reduced, without making fabric resistance a significant contributor to pressure drop. The GORE-TEX® fabric allows for this optimization by providing a microfine pore structure while maintaining sufficient fabric permeability to permit operation at high air-to-cloth (A/C) ratios. A measure of the new fabric permeability is the Frazier number which is the volume of gas that will pass through a square foot of fabric sample at a pressure drop of 0.5 in. W.C. (0.12 kPa). The Frazier number of the bags for the Phase III tests is in the range from 4 to 8 ft/min (1.22 to 2.44 m/min). Through the filter, viscous (laminar) flow conditions exist, so the pressure drop varies directly with flow velocity. Assuming a new fabric Frazier number of 6 ft/min (1.8 m/min), the pressure drop across the fabric alone would be 1.0 in. W.C. (0.25 kPa) at an A/C ratio (filtration velocity) of 12 ft/min (3.7 m/min).

The second term in Eq. 1 accounts for the pressure drop contribution from the permanent residual dust cake that exists on the surface of the fabric. For operation at high A/C ratios, the bag cleaning must be sufficient to maintain a very light residual dust cake and ensure that the pressure drop contribution from this term is reasonable. The contribution to pressure drop from this term is one of the most important indicators of longer-term bag cleanability.

The third term in Eq. 1 accounts for the pressure drop contribution from the dust accumulated on the bags since the last bag cleaning. K_2 is determined primarily by the fly ash particle-size distribution and the porosity of the dust cake. Typical K_2 values for a full dust loading of pulverized coal (pc)-fired fly ash range from about 4 to 20 in. W.C.-ft-min/lb (0.5 to 2.5 kPa-m-min/kg), but may, in extreme cases, cover a wider range. Within this term, the bag-cleaning interval, t, is the key performance indicator. The goal is to operate with as long of a bag-cleaning interval as possible, since more frequent bag pulsing can lead to premature bag failure and requires more energy consumption from compressed air usage. For Phase III, the stated goal was to operate with a pulse interval of at least 10 min while operating at an A/C ratio of 12 ft/min (3.7 m/min).

Total tube sheet pressure drop is another key indicator of overall performance of the AHPC. Here, the stated Phase III goal was to operate with a tube sheet pressure drop of 8 in. W.C. (2.0 kPa) at an A/C ratio of 12 ft/min (3.7 m/min). Note that the average pressure drop is not the same as the pulse-cleaning trigger point. For many of the previous and current tests, the pulse trigger point was set at 8 in. W.C. (2.0 kPa), but the average pressure drop was significantly lower.

To help analyze filter performance, the terms in Eq. 1 can be normalized to the more general case by dividing by velocity. The dP/V term is commonly referred to as drag or total tube sheet drag, D_T.

$$\frac{dP}{V} = D_T = K_f + K_2 W_R + \frac{K_2 C_i V t}{7000} \qquad \text{[Eq. 2]}$$

The new fabric drag and the residual dust cake drag are typically combined into a single term called residual drag, D_R.

$$D_T = D_R + \frac{K_2 C_i V t}{7000} \qquad \text{[Eq. 3]}$$

The residual drag term then is the key indicator of how well the bags are cleaning over a range of A/C ratios, but may still be somewhat dependent on A/C ratio. For example, it may be more difficult to overcome a dP of 10 in. W.C. (2.5 kPa) to clean the bags than cleaning at a dP of 5 in. W.C. (1.25 kPa). For most baghouses, the residual drag typically climbs somewhat over time and must be monitored carefully to evaluate the longer-term performance.

Between bag cleanings, from the second term in Eq. 3, the drag increases linearly with K_2 (dust cake resistance coefficient), C_i (inlet dust concentration), V (filtration velocity), and t (filtration time). For conventional baghouses, the C_i term is easily determined from an inlet dust loading measurement, and approximate K_2 values can be determined from the literature or by direct measurement. However, for the AHPC, the concentration of the dust that reaches the bags is generally not known and would be very difficult to measure experimentally. From the Phase I laboratory tests, results indicated approximately 90% of the dust was precollected and did not reach the fabric. However, this amount is likely to fluctuate significantly with changes to the electrical field and with the dust resistivity. Since C_i is not known, for evaluation of AHPC performance, the K_2 and C_i can be considered together:

$$K_2 C_i = \frac{(D_T - D_R)\ 7000}{Vt} \qquad \text{[Eq. 4]}$$

Evaluation of K_2C_i can help in assessing how well the ESP portion of the AHPC is functioning, especially by comparing with the K_2C_i during short test periods in which the ESP power was shut off.

Eq. 4 can be solved for the bag-cleaning interval, t, as shown in Eq. 5. It is clear that the bag-cleaning interval is inversely proportional to the face velocity, V, and the K_2C_i term and directly proportional to the change in drag before and after cleaning (delta drag). The delta drag term is dependent on the cleaning set point or maximum pressure drop as well as the residual drag. The face velocity, delta drag, and K_2C_i terms are relatively independent of each other and should all be considered when the bag-cleaning interval is evaluated. However, as mentioned above, the drag may be somewhat dependent on velocity if the dust does not clean off the bags as well at high velocity as at low velocity. Similarly, the K_2C_i is somewhat dependent on velocity

for a constant plate collection area. At the greater flow rates, the SCA of the precipitator is reduced, which will result in a greater dust concentration, C_i, reaching the bags.

$$t = \frac{(D_T - D_R)\,7000}{VK_2C_i} \qquad \text{[Eq. 5]}$$

4.0 AHPC RESULTS FROM BIG STONE

4.1 Analysis of Bag-Cleaning Interval

Initial results, reported in the April–June Quarterly Report, showed that the AHPC with the modified configuration exceeded the performance goals of a 10-min bag-cleaning interval at an A/C ratio of 12 ft/min (3.7 m/min) and 8-in. W.C. (2.0-kPa) pressure drop. During July, further tests at Big Stone were completed to help establish the relationships among pressure drop, bag-cleaning interval, and A/C ratio.

Big Stone power plant was in a very stable operating condition during the whole test period with a typical gross load of 450 MW and an ESP inlet temperature of 300°F (149°C), except for an unplanned outage on July 16.

The AHPC was brought on-line on June 28 with an A/C ratio of 10 ft/min (3.05 m/min) and a pulse trigger pressure of 7.0 in. W.C. (1.74 kPa) and multibank pulsing through July 5. The purpose of these parameters was to compare results with previous operation at a pulse trigger set point of 8 in. at an A/C ratio of 12 ft/min (3.7 m/min). The daily average pressure drop and the corresponding residual drag from June 28 to July 5 are plotted in Figures 1 and 2. The average pressure drop started at 6.0 in. W.C. (1.5 kPa) on June 28, and then remained steady at 6.5 in. W.C. (1.63 kPa) at an A/C ratio of 10 ft/min (3.05 m/min). The residual drag demonstrated the same trend, initially at 0.3 in. W.C./ft/min (0.25 kPa/m/min), and reaching a steady condition ranging from 0.55 to 0.62 in W.C./ft/min (0.45–0.50 kPa/m/min) due to the seasoning of the bags. The bag-cleaning interval ranged from 7 to 35 min as shown in Figure 3. K_2C_i, calculated as a function of bag-cleaning interval is shown in Figure 4. A reasonably long bag-cleaning interval, ranging from 10 to 35 min, was observed when K_2C_i was less than 8. These results demonstrated it was possible to have lower average pressure drop and longer bag-cleaning interval with a small decrease in A/C ratio.

Further short-term tests were carried out after July 6 to evaluate the effects of A/C and pulse trigger pressure drop on AHPC performance. The high voltage (HV) power was also shut down several times to investigate the relationship between bag-cleaning interval and K_2C_i.

During the test on July 7, the A/C ratio was maintained at 8 ft/min (2.44 m/min) until 9:00 p.m., when the A/C was set at 10 ft/min (3.05 m/min). The pulse trigger pressure was set to 5.5 in. W.C. (1.38 kPa) from 12:00 a.m. to 9.00 a.m. and then changed to 7.5 in. W.C. (1.88 kPa) for the rest of the test period. The resultant pressure drop and bag-cleaning intervals are plotted in Figures 5 and 6. It is seen that, under the same A/C ratio (8 ft/min [2.4 m/min]), the

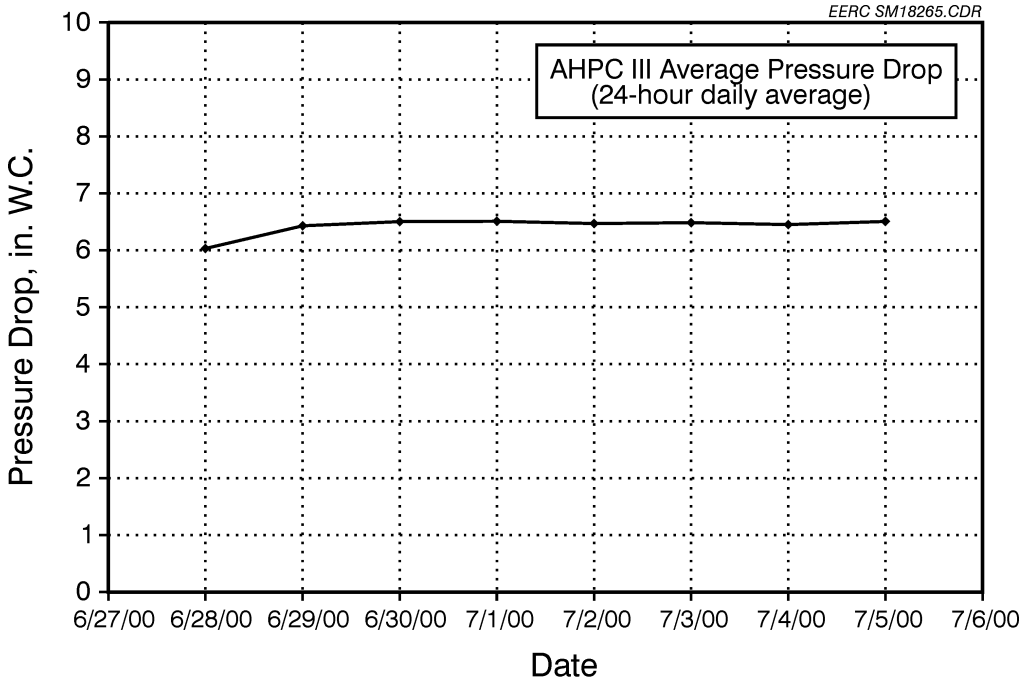

Figure 1. Daily average pressure drop for June 28–July 5.

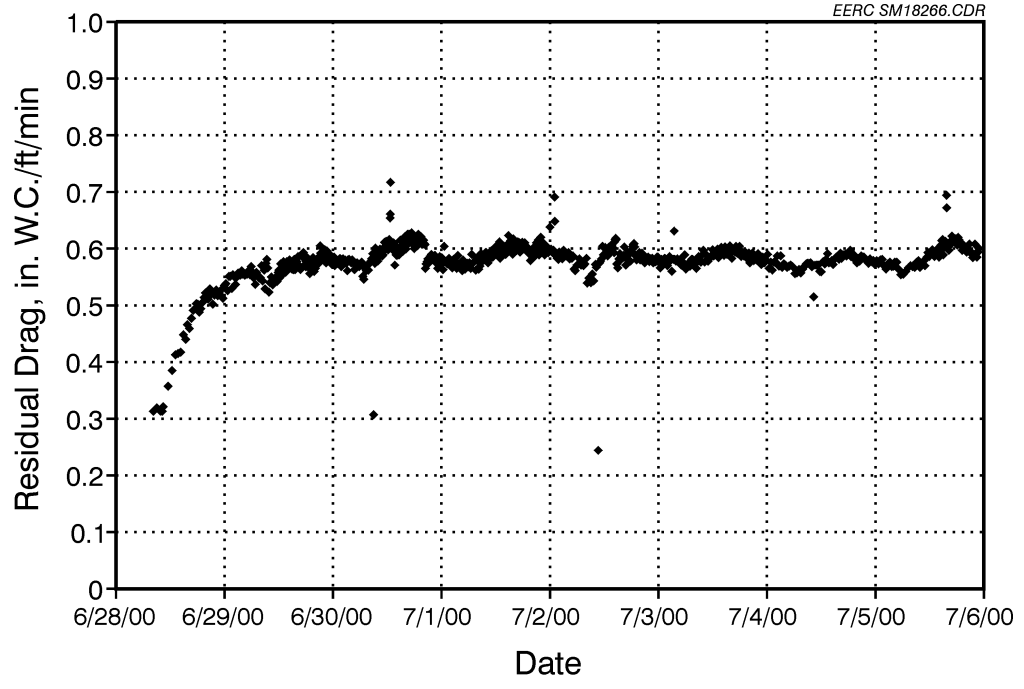

Figure 2. Residual drag for June 28–July 5.

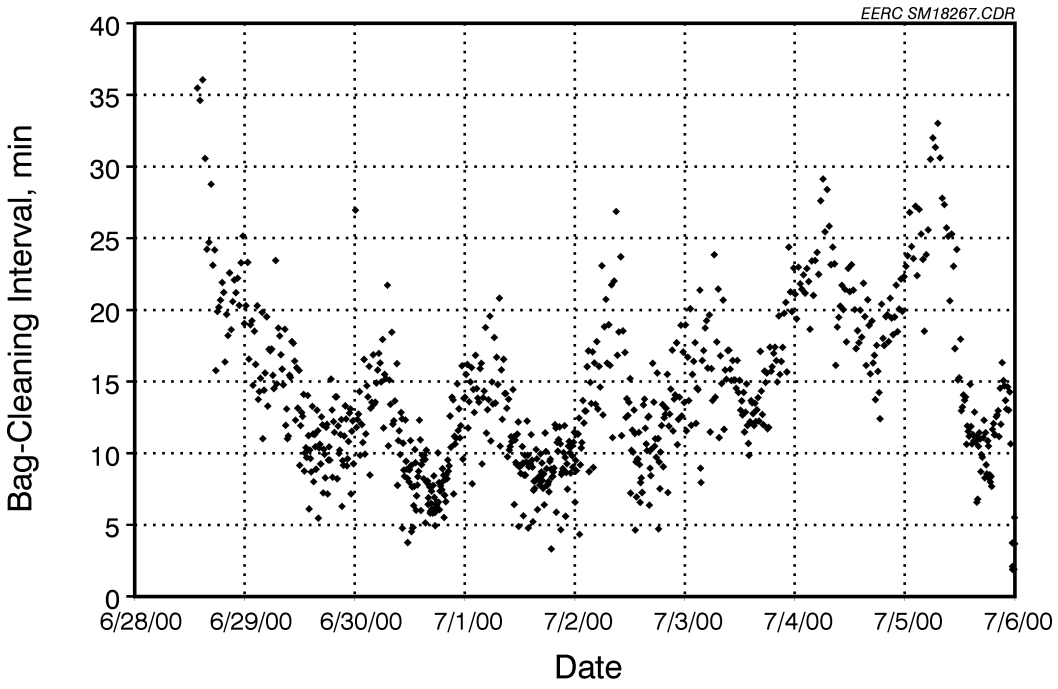

Figure 3. Bag-cleaning interval for June 28–July 5.

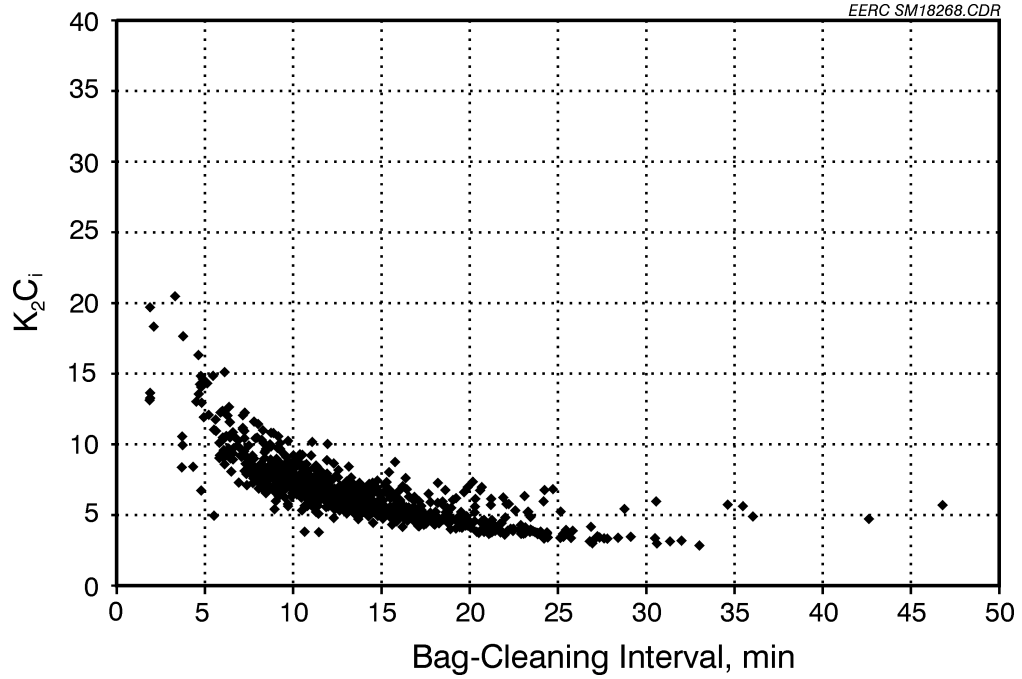

Figure 4. K_2C_i as a function of bag-cleaning interval for June 28–July 5.

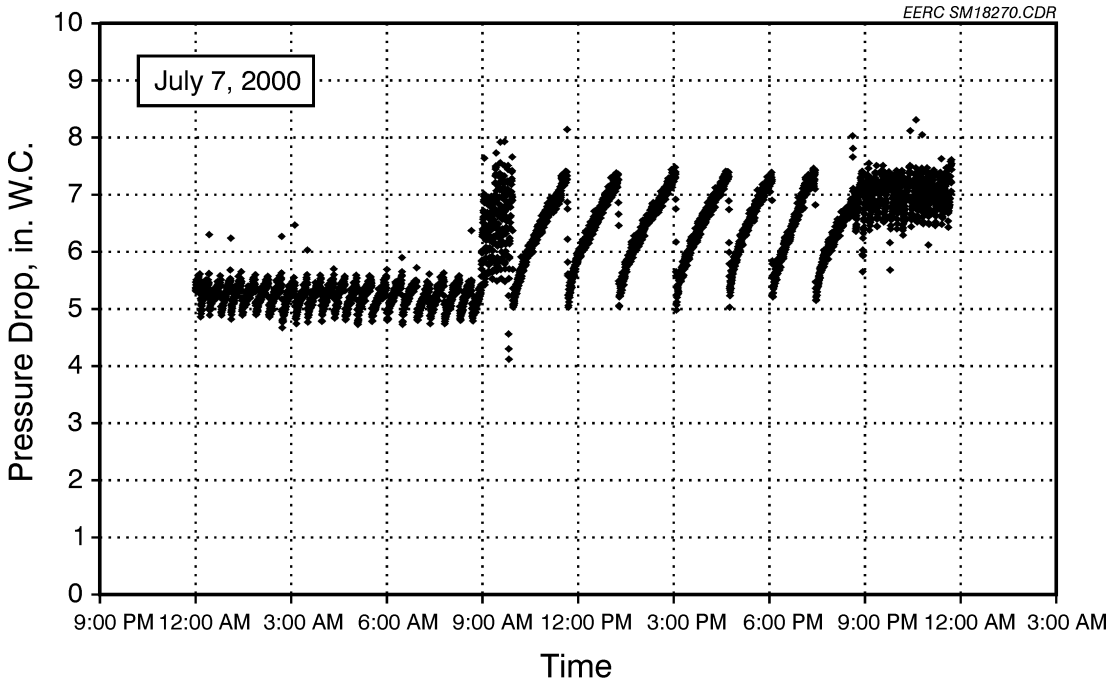

Figure 5. Pressure drop for July 7.

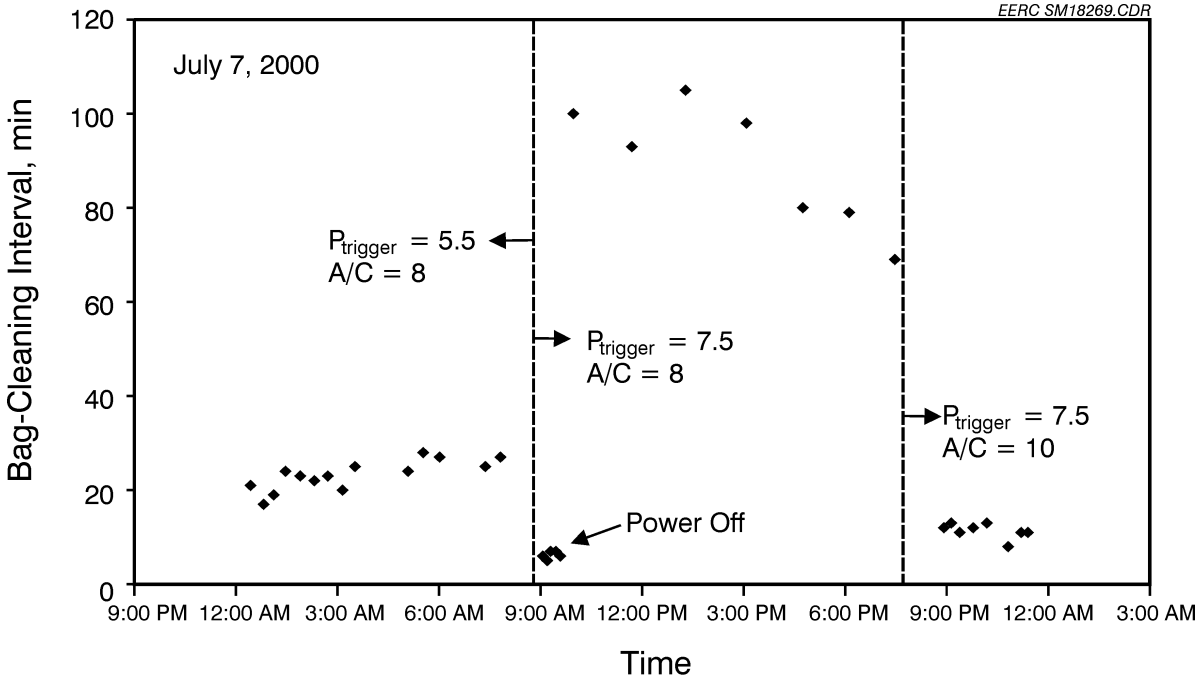

Figure 6. Bag-cleaning interval for July 7.

bag-cleaning interval increased significantly from around 20 min at a pulse trigger pressure of 5.5 in. W.C. (1.38 kPa) to 80–100 min at the higher pulse trigger pressure of 7.5 in. W.C. (1.88 kPa). The observed reduction of bag-cleaning interval to 5–7 min at 9:30 a.m. was due to the scheduled shutdown of HV power at that time. When the A/C ratio was increased to 10 ft/min (3.05 m/min) at 9:00 p.m., at a pulse trigger pressure of 7.5 in. W.C. (1.88 kPa), the bag-cleaning interval dropped to 11–13 min. The calculated K_2C_i was plotted as a function of time in Figure 7. The high values of K_2C_i up to 45 were observed when the HV power was off because all of the fly ash particles went toward the bags. When pulse trigger pressure was switched from 5.5 in. W.C. (1.38 kPa) to 7.5 in. W.C. (1.88 kPa) at a constant A/C ratio of 8 ft/min (2.4 m/min), except for the test period when the HV power was shut off, K_2C_i was slightly decreased with the increasing difference in ΔP before and after bag cleaning, as shown in Figure 8. Assuming a constant C_i during that test period, it is concluded that K_2 is inversely proportional, to some extent, to the ΔP difference before and after bag cleaning. The bag-cleaning interval was plotted as a function of K_2C_i as shown in Figure 9. The bag-cleaning interval is inversely proportional to K_2C_i ($t \propto (K_2C_i)^{-0.77}$), demonstrating that even a small reduction of K_2C_i when K_2C_i is smaller than 5 resulted in a significant increase of bag-cleaning interval.

The A/C ratio from July 9 at 12:00 p.m. to July 10 at 12:00 a.m., shown in Figure 10, was set at 6, 8, and 10 ft/min (1.83, 2.44, and 3.05 m/min), and the pulse trigger was set at 6, 6.5, and 7.5 in. W.C. (1.5, 1.63, and 1.88 kPa) during the test period. The resultant pressure drop and the bag-cleaning interval are plotted in Figures 11, and 12. The bag-cleaning interval increased significantly from around 10 min at the A/C of 10 ft/min (3.05 m/min) and 7.5 in. W.C. (1.88 kPa) pulse trigger to 120 min at an A/C ratio of 6 ft/min (1.83 m/min) and a pulse trigger of 6 in. W.C. (1.5 kPa). At an A/C of 8 ft/min (2.44 m/min) and a pulse trigger of 7.5 in W.C. (1.88 kPa), the interval was 100 min, but it was reduced to 50–60 min when the pulse trigger was

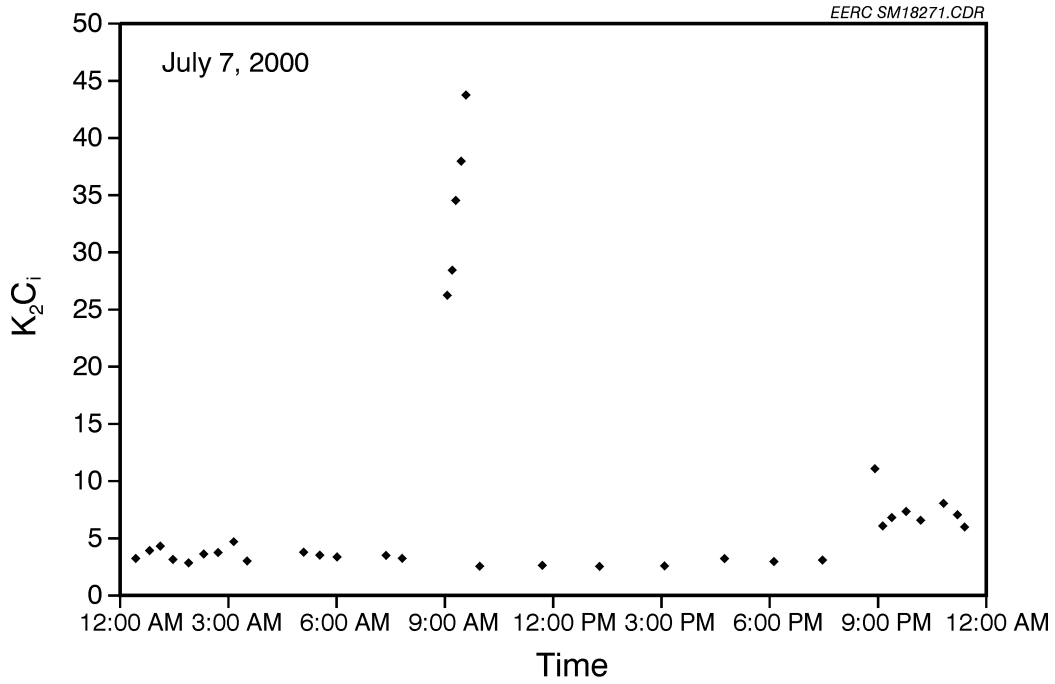

Figure 7. K_2C_i for July 7.

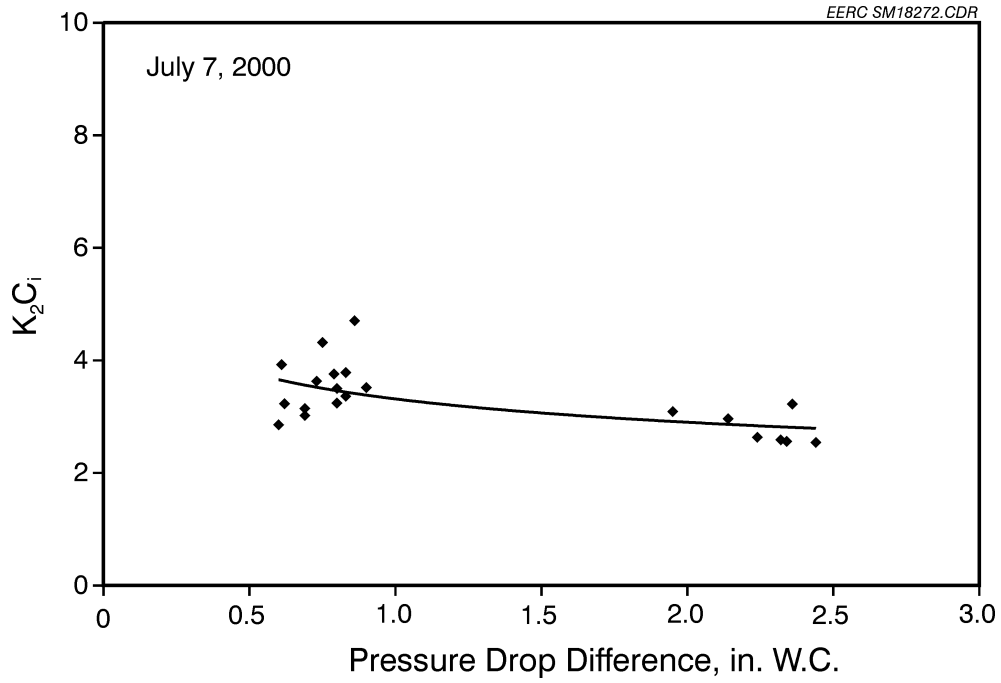

Figure 8. K_2C_i versus difference in pressure drop before and after bag cleaning for July 7.

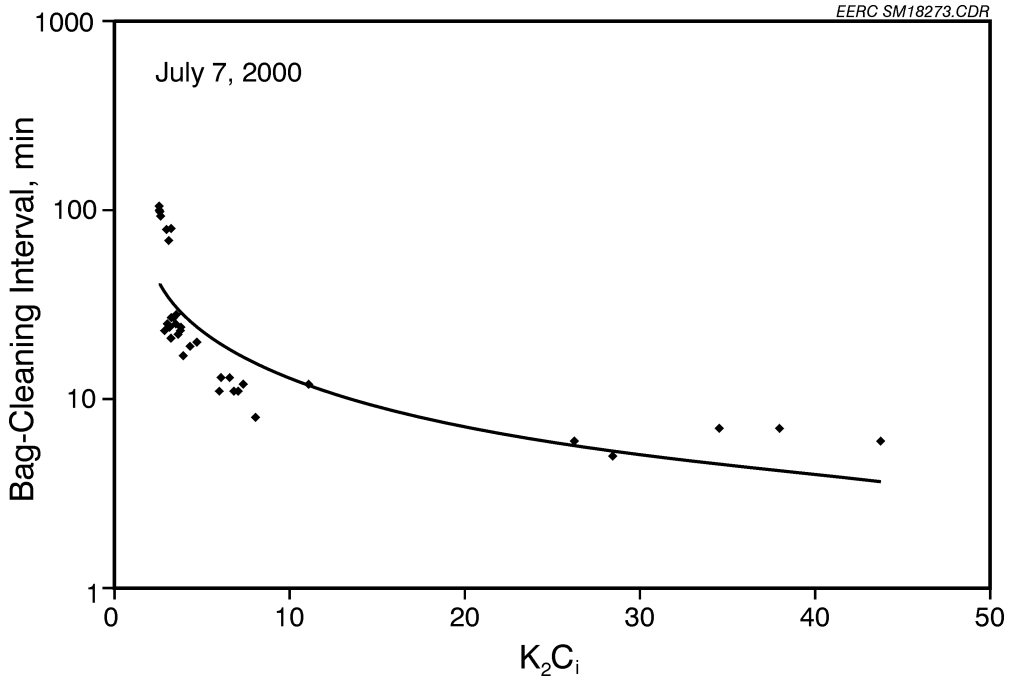

Figure 9. Bag-cleaning interval versus K_2C_i for July 7.

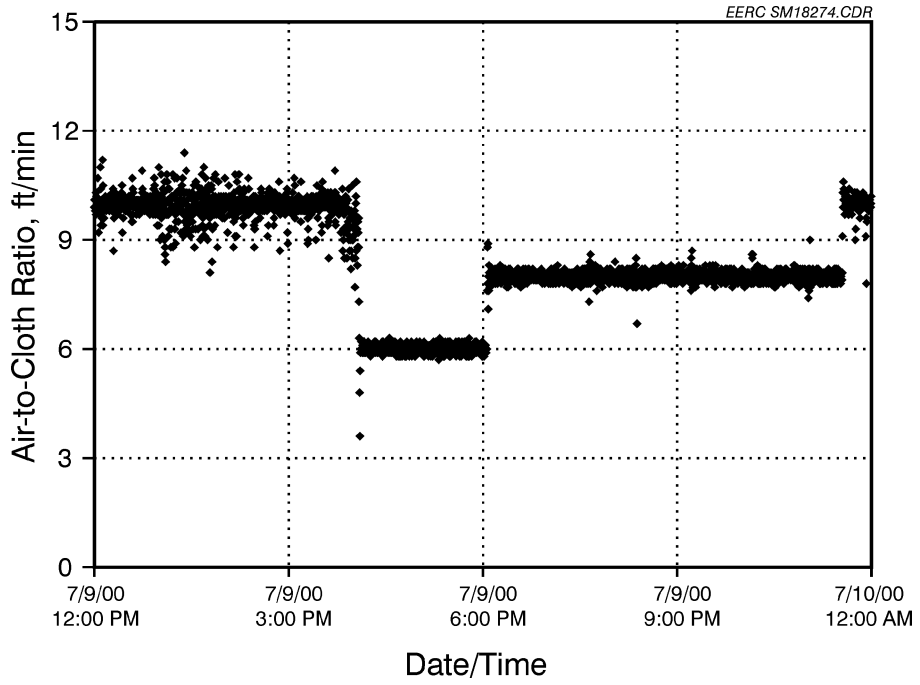

Figure 10. A/C ratio for July 9.

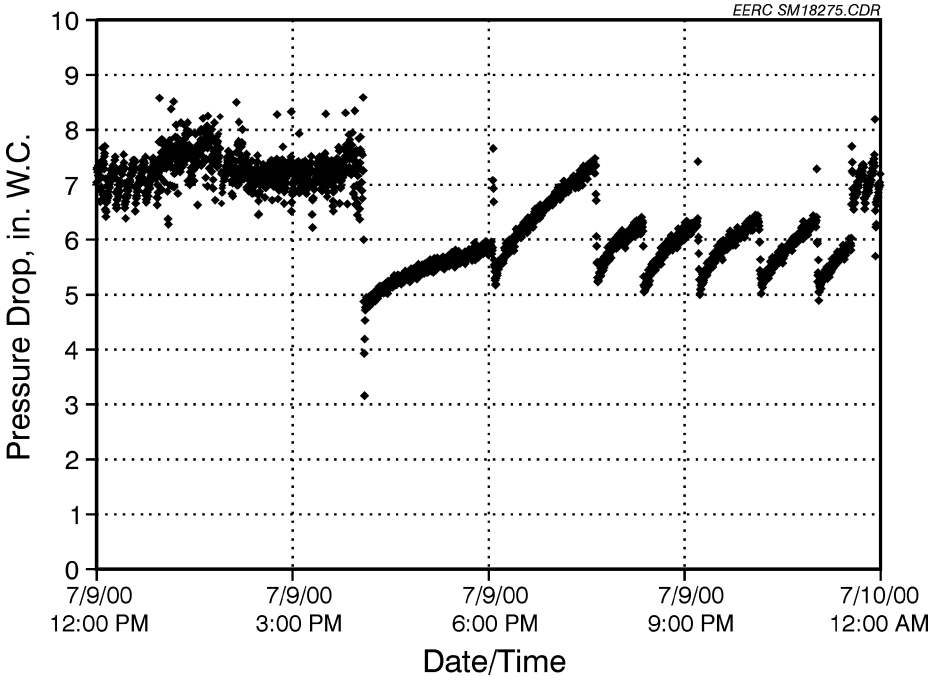

Figure 11. Pressure drop for July 9.

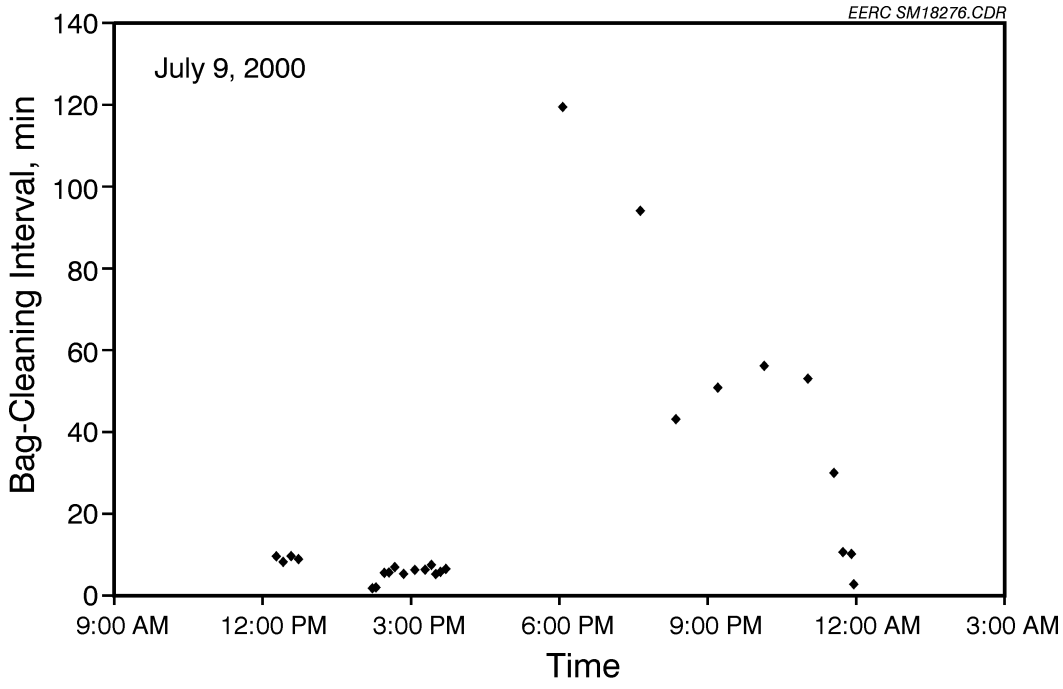

Figure 12. Bag-cleaning interval for July 9.

reduced to 6.5 in. W.C. (1.63 kPa) while the A/C ratio was held constant. The K_2C_i was calculated and plotted as a function of the bag-cleaning interval, as shown in Figure 13. The approximately inverse dependence of bag-cleaning interval on K_2C_i ($t \propto (K_2C_i)^{-0.55}$) is demonstrated again.

4.2 AHPC Model Modification

Results show that the bag-cleaning interval can be controlled by adjusting A/C ratio and pulse trigger pressure, which is in agreement with the theoretical expectation, discussed in the previous quarterly report.

The theoretical dependence of bag-cleaning interval was presented in Section 3 of this report. Based on the experimental results from Big Stone Power plant, the relationship between bag-cleaning interval and K_2C_i can be described as:

$t \propto (K_2C_i)^{-\alpha}$, $(1 > \alpha > 0)$

The value of α is not described in the theory (Eq. 5), but may be the result of the complex particle transport in the AHPC, when both electrostatic precipitation and filtration occur simultaneously.

The ESP particulate collection efficiency has been widely studied and well established as:

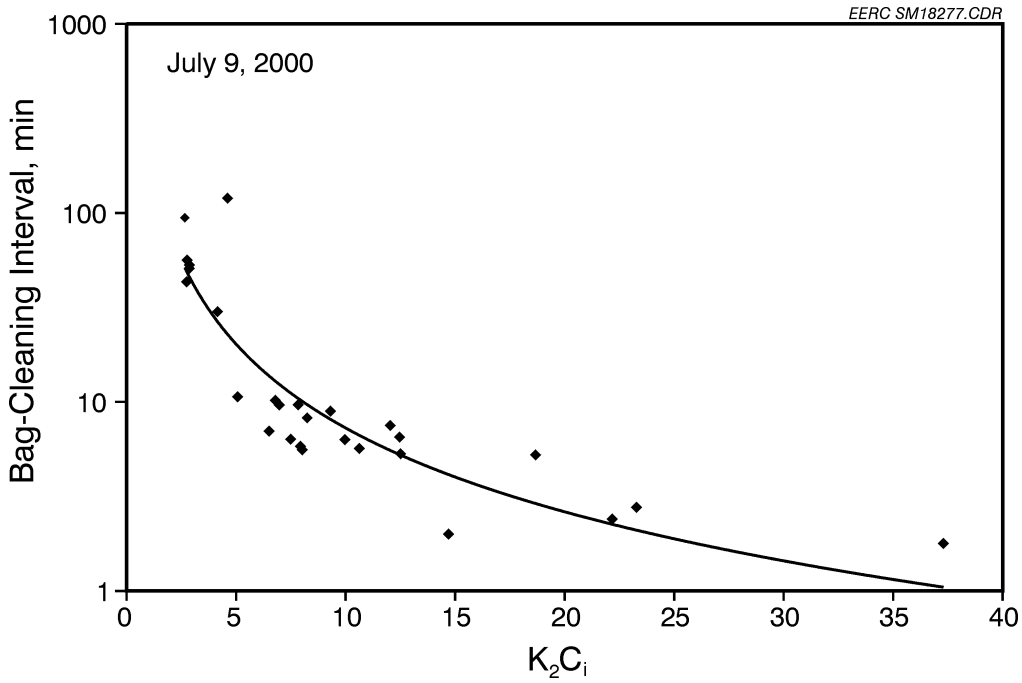

Figure 13. K_2C_i versus bag-cleaning interval for July 9.

$$C_i = C_0 \exp\left(\frac{-2 \cdot L \cdot V_e}{b \cdot V}\right) \qquad \text{[Eq. 6]}$$

where C_0 is the inlet dust loading for the AHPC or an ESP; L is the length of the ESP; b is the plate spacing of the ESP; V_e is the electric migration velocity of fly ash particles; V is the flue gas velocity; and C_i is the outlet dust loading of the ESP or the dust loading to the bags. By combing L, b, and V_e together, effective migration velocity (ft/min) is defined as:

$$V_e' = \frac{-2 \cdot L \cdot V_e}{b} \qquad \text{[Eq. 7]}$$

Equation 6 is transformed as:

$$C_i = C_0 \exp\left(\frac{V_e'}{V}\right) \qquad \text{[Eq. 8]}$$

Considering the complex geometric configuration of AHPC, flow turbulence, and other nonideal factors, the accurate effective migration velocity, V_e', is difficult to determine. However, experimental results in Phase I indicated at least 90% of the dust was precollected and did not reach the fabric under normal operating conditions. Therefore, an estimation of effective migration velocity of 13 ft/min (3.96 m/min) was made, resulting in 11.4% of total fly ash moving to the bags at a face velocity of 6 ft/min (1.83 m/min). Equation 5 is then changed as:

$$t = \frac{7000\left(\Delta P_T - \Delta P_R\right)}{V^2 K_2 C_0 \exp\left(\frac{-13}{V}\right)} = \frac{7000\left(\Delta D_T - \Delta D_R\right)}{V K_2 C_0 \exp\left(\frac{-13}{V}\right)} \quad \text{[Eq. 9]}$$

From the above field studies on Big Stone power plant, it is noted that K_2 is somewhat a function of face velocity as well as pressure drop across the bags. Experiments were carried out when the HV power was shut off to investigate the behavior of K_2 by adjusting face velocity and pressure drop, and the results are shown in Table 1. Under this condition, the AHPC operated as a high-ratio baghouse. By assuming a typical ESP inlet dust loading of 2.35 grains/acf, K_2 was calculated and is also shown in Table 1. The calculated K_2 at the same ΔP difference of approximately 2 in. W.C. (0.5 kPa) plotted as a function of face velocity, shown in Figure 14, indicated a dependence of K_2 on velocity roughly on the order of 0.768.

TABLE 1

Experimental Results (AHPC HV power off)

ΔP max., in. W.C.	ΔP min., in. W.C.	ΔP Difference, in. W.C.	AC, ft/min	t, min	delta drag, in. W.C./ft/min	K_2, in. W.C.·ft ·min/lb
6	4.2	1.93	6.00	12.5	0.3	12.77
8	4.11	3.84	6.00	27	0.6	11.77
7	3.99	2.84	6.00	23	0.5	10.22
8	5.5	2.25	8.00	6	0.3	17.45
8	5.75	2.25	8.00	9	0.3	11.64
8	6.73	0.99	10.00	2	0.1	14.74
8	7.45	0.87	10.00	1.78	0.1	14.56
8	7.37	0.71	10.00	1.8	0.1	11.75
9	6.72	2.27	10.00	4	0.2	16.90

In order to clarify the roles of pressure drop before and after cleaning and face velocity on bag-cleaning interval, experimental data are summarized in Table 2. Based on the previous assumptions, i.e., inlet dust loading of 2.35 grains/acf, an effective velocity of 13 ft/min (3.96 m/min) with an initial estimation on relationship between $K_2 \propto V^{0.768}$, and by using a least squares method, a semiempirical equation is proposed as:

$$t = \frac{7000\left(\Delta P_T - \Delta P_R\right)^{1.548} 0.123}{V^{2.1} C_0 \exp\left(\frac{-13}{V}\right)} \quad \text{[Eq. 10]}$$

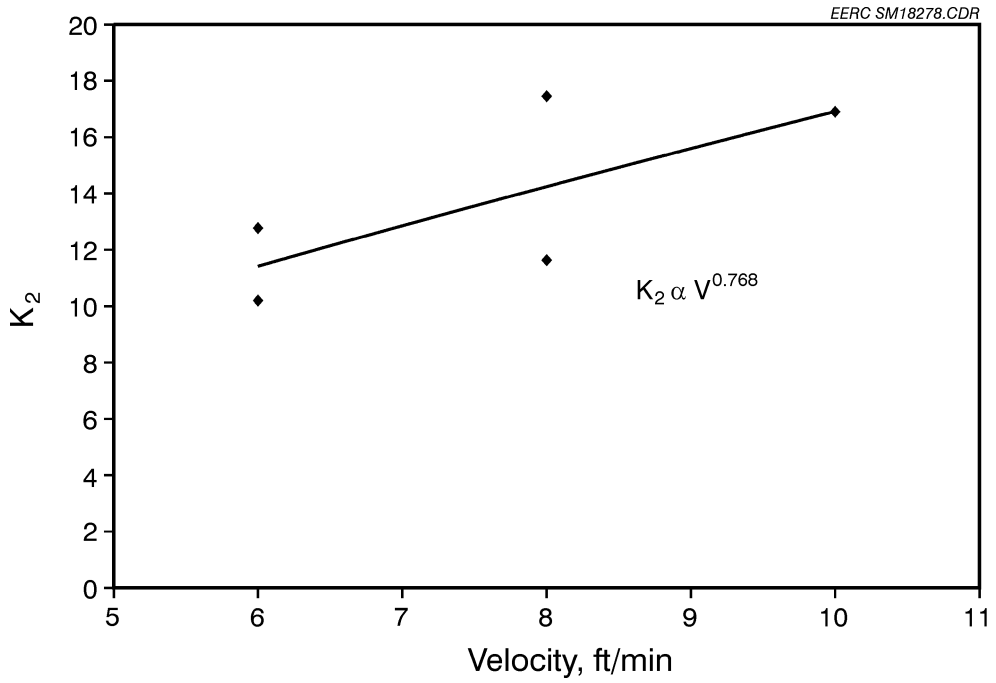

Figure 14. K_2C_i versus velocity.

TABLE 2

Experimental Results and the Predicted Time Interval under Normal AHPC Performance

ΔP max., in. W.C.	ΔP min., in. W.C.	ΔP Diff., in. W.C.	AC, ft/min	Actual t, min	Predicted t, min
4.98	3.64	1.3	6	120	106
4.41	3.57	0.8	6	45	52
4.18	3.7	0.5	6	14.8	23
5.5	4.67	1.0	8	25	18
7.5	5.0	2.5	8	98	94
5.5	4.88	0.6	8	14	12
7.5	5.15	2.4	8	92	85
6.5	5.0	1.5	8	51	44
7.5	6.45	1.1	10	12	12
7	5.92	1.1	10	20	13
7.5	6.15	1.4	10	13.5	18
8	6.8	1.2	10	14	15
8	5.8	2.2	10	25	38

Predicted bag-cleaning interval under experimental conditions was plotted versus real bag-cleaning interval as shown in Figure 15. More than 70% of experimental data fall within ±30%, with an average error of 20.8%. By comparing with the theoretical Equation 10, it shows $K_2 \propto \triangle P^{-0.548} V^{0.1}$, which qualitively agreed with the observation in the field study, implying that ΔP has a strong influence on K_2 compared with face velocity.

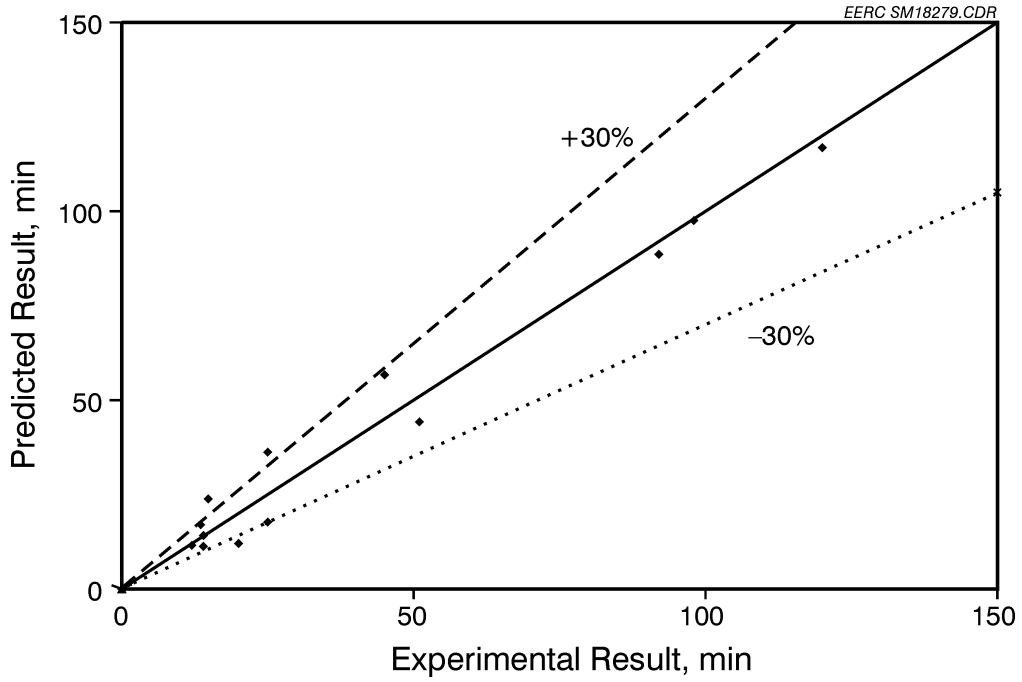

Figure 15. Comparison of predicted time interval with experimental results.

5.0 FILTER BAG EVALUATION

GORE-NO STAT® filter bags were installed and precoated with the fly ash dust from the Big Stone plant ESP prior to start-up of the AHPC Phase III testing on April 18, 2000.

The filter bags contain an electrically conductive ePTFE (expanded polytetrafluoroethylene) fiber. The conductive felt fibers help to dissipate electrical charge buildup across the surface of the filter bags. A filter media that can dissipate charge is desirable in the AHPC because of the presence of electrical charges on the dust or in the gas.

The filter media is also required to withstand the high-temperature and corrosive conditions encountered in many coal-fired boiler fabric filter dust collectors. GORE-NO STAT® fiber felt is chemically inert and can withstand continuous operating temperatures as high as 500°F (260°C). The ePTFE fibers have excellent chemical resistance to mineral and organic acids, alkalies, oxidizing agents, and organic solvents.

During the first 2 months, operating parameters were varied, and the power plant coal source changed a number of times. Several unscheduled maintenance outages and a planned annual outage subjected the AHPC to system upsets. The unscheduled Big Stone boiler shutdowns resulted in immediate loss of airflow and power to the AHPC, and the subsequent restarts may have exposed the bags to flue gas dew point excursions.

Seven filter bags were removed from the AHPC unit for inspection and analysis on June 27, after 1360 hr of operation. New filter bags replaced the ones removed in June. On July 21, additional filter bag inspection included one of the new bags that had been installed in June.

The operation of the filter bags in the Phase III testing was undertaken with a new AHPC configuration and new components as described in the previous quarterly report. AHPC testing was stopped on May 5 to 8 for an unscheduled power plant outage, on May 17 to 30 for Big Stone's annual maintenance outage, and again on June 27 for filter bag inspection. The shutdown procedure followed for the maintenance outage and filter bag inspection included cleaning bags on-line and off-line to remove the dust cake from the bag surface. In addition, the filter bags were precoated with fly ash from the ESP hopper prior to start-up after the outage. Seven bags were returned to W.L. Gore & Associates, Inc. (Gore), for lab analysis from the following locations: Row 3/Bag 3-(R3B3), R3B6, R4B4, R4B7, R2B1, R2B2, and R1B5. For reference, the location of Row 1 is closest to the collector flue gas outlet pipe side, and Bag 1 is closest to the pulse system manifold and valve side.

5.1 Visual Analysis

All seven filter bags contained a thin layer of dust on the membrane surface, typical of most coal-fired boiler applications. The primary dust cake was easily brushed off and revealed a membrane that looked white with 0.4- to 0.12-in. (10- to 3-mm)-diameter dust nodules interspersed on the membrane surface along the entire length and circumference of the filter bags. A larger concentration of nodules was found 7 to 10 in. (0.18 to 0.25 m) from the top and then from 24 in. (0.61 m) to the bottom of the filter bags. A photograph was taken at 17× magnification of Row 2/Bag 2's surface after light brushing (see Figure 16) showing the nodules. Past experience has shown nodules are an indication that the filter bags were exposed to flue gas dew point excursions similar to what may have occurred during the unscheduled outage. Using the fly ash from the new coal types as a precoat may have contributed to the formation of the nodules. The hygroscopic properties of fly ash vary with its properties and type. When exposed to moisture during flue gas temperature excursions, nodules can form on the filter bags. In the past, this problem was not seen on the previously used coal. After this filter bag evaluation, new procedures were implemented to correct the problem. The new procedure requires precoating the bags with crushed limestone prior to start-up. The limestone acts to absorb the moisture and unlike some fly ash does not form a cementitious nodule to adhere to the surface of the bag. After the filter bag is cleaned, the limestone is removed, and the bag resumes normal operation at the now-appropriate temperature and operating conditions.

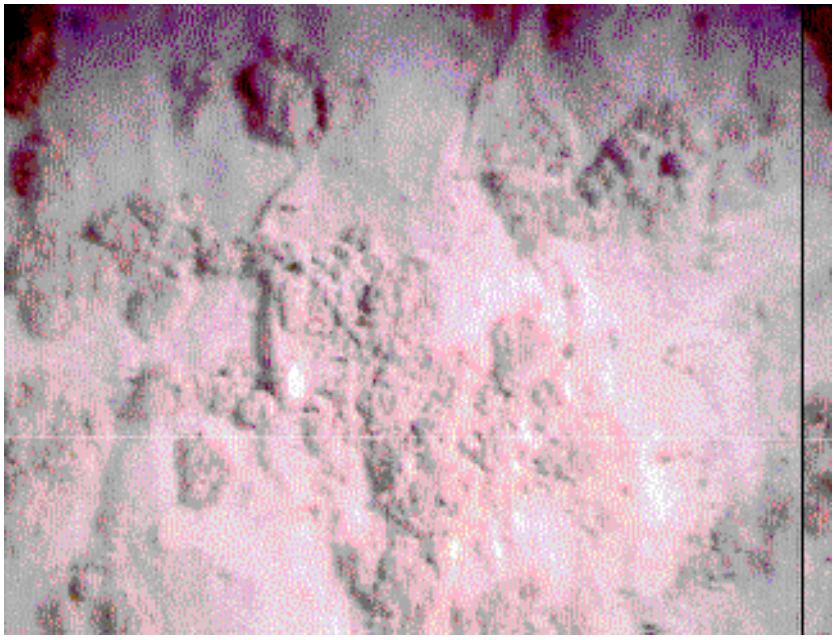

Figure 16. Row 2 Bag 2 after brushing.

The filter bags were examined for membrane damage from sparking, high flue gas velocity abrasion, chemical/temperature degradation, and possible pulse-jet overcleaning. There was no indication of membrane damage from abrasion, temperature, or chemical attack.

On most of the filter bags inspected, membrane damage was observed along two areas of the filter bag that began 24 to 27 in. (0.61 to 0.69 m) from the top of the bag and extended to the bottom of the bag. The majority of visual damage was located along the vertical cage wires that were adjacent to the position of the discharge electrodes. Typically, the damage occurred along four of the twelve cage wires, two groups of two on opposite sides of the filter bag that were closest to the discharge electrodes. The observations of small holes 0.02–0.08 in. (0.5–2 mm) in diameter and their location indicate the possibility of some type of electrically induced damage.

The bags in positions in the rear of the AHPC opposite the inlet had greater damage. The bags at the inlet had very little to no damage. The major operating difference between these two sections is the presence of extreme back corona from the collecting plates in the back of the AHPC due to heavy deposits of dust on the plates from ineffective cleaning or rapping of the plates.

The location of the damage close to the discharge electrodes indicates that back corona may have occurred between the discharge electrodes and filter bags. During testing, numerous visual observations through the site ports were made during both daytime and nighttime hours of the interior of the AHPC to evaluate discharge electrode corona intensity and collecting plate back corona intensity and location. Several engineers and operators observed electrode corona discharge toward the plate and back corona at several locations on the plate. No sparking to or back corona from the filter bags was observed. The conductive felt is designed to dissipate the

charge buildup on the surface of the bags as well as keep the filter media conductive and reduce any voltage drop across it. Since the membrane damage occurred along the cage wires directly opposite the discharge electrodes and no sparking to the bags was observed, back corona is the suspected cause of the damage. However, the lack of visibility of back corona from the bags indicates the back corona may be very weak, yet possibly able to damage the bags.

On July 21, 2000, the AHPC operation was idled to remove and inspect Row 4/Bag 7, which had been installed on June 26, 2000. The filter bag after 670 hr of operation had a thin layer of dust present that was easily brushed off. Similar observations were made on this bag as on the aforementioned bags. Membrane damage was observed in the middle and bottom of the bag along the vertical cage wires closest to the discharge electrodes. At the bottom, some membrane damage occurred between the cage wires. There was no membrane damage in the top 28 in. (0.71 m) of the filter bag. This is another important point. While the discharge electrode masts start at a point 10 in. (0.25 m) below the tube sheet, the directional corona discharge tabs of the electrodes start at a point 28 in. (0.71 m) below the tube sheet in the exact vertical location the bag damaged started. This suggests that the bag damage is related to the corona discharge location and possible electric field effects as the dust is charged and collected on the plate just opposite of the bags.

5.2 Media Analysis

Laboratory analysis of the chemical and elemental material properties of the damaged membrane areas was carried out on two of the filter bags along with a brand new one for comparison purposes. Row 3/Bag 6's membrane surface was analyzed at the top and along a vertical cage wire. The results indicate the remaining dust on the membrane surface is made up of inorganic sulfate, aluminum, calcium, magnesium, sodium, and silicon which would all be expected in fly ash. The Row 2/Bag 1 surface was also analyzed at the middle and on the cuff bottom where a small portion of the cuff was blackened. The media analysis reveals a breakdown in the chemical structure of the ePTFE membrane at the location where the damage is noted. This is usually due to high temperatures. Because the damage was localized on the media, the effects are not the result of flue gas temperature excursions. The media breakdown is likely the result of electrical spark or back corona-induced high-temperature effects. The small areas of damage localized near the cage wires did not result in evidence of increased emissions as indicated by the spotless condition of the clean air plenum when the bags were removed.

Additional testing is being conducted to investigate this media damage. The changes in the design of the AHPC from Phase II to Phase III included new discharge electrodes, new plates, smaller spacing between the bags, and discharge electrodes. One or several of these may have contributed to the media damage.

5.3 Dimensional Analysis

The flat width of the bags was 9.02 to 9.21 in. (0.229 to 0.234 m) as measured in the lab after 8 weeks of operation. The bag width of new bags was measured as 9.02 in. (0.229 m). All

the bags were cut and manufactured to the identical flat-width specifications. The bags have maintained their dimensional stability during the 8 weeks of operation.

5.4 Air Permeability Analysis

The air permeability analysis of the AHPC filter bag media was performed in the lab using the Frazierometer. This device measures the amount of air that flows through a flat sample of media 3.5 in. (0.09 m) in diameter and correlates it to a Frazier number. The Frazier number describes the volume of air (cfm) passing through 1 square foot of media at a differential pressure of 0.5 in. W.C. (0.125 kPa). This is expressed as 1.0 Frazier equals 1 cfm/sq. ft. at 0.5 in. W.C. (0.125 kPa), canceling units of sq. ft.; the Frazier number units are expressed as ft/min at 0.5 in. W.C. (0.125 kPa).

Samples of the AHPC filter bag media were cut from the top, middle, and bottom bag locations. The sample size was 5 in. (0.127 m) in vertical bag length direction along the entire circumference of the bag. This enables three measurements to be taken per bag location. The test produces a total of nine data points for each filter bag. A sample is tested for permeability in the condition it was received from the field application and labeled (as received). The nine readings are then averaged to create a bag permeability number.

Additional testing of the same samples is completed to determine the permeability condition of the membrane. A very soft brush is used to lightly remove the dust particles on the surface of the membrane. Care is taken to prevent brushing the dust into the membrane or smearing the dust cake across the surface. The permeability of the samples is tested to make sure the test heads match up exactly with the test area previously measured. An average of the nine measurements is compared to the new permeability of the media for changes in condition and as an indicator for performance.

The data from the seven bags are displayed in Table 3. As a baseline, the new Frazier number of the media used in Phase III tests is within the range of 4.0 to 8.0 ft/min at 0.5 in. W.C. (0.125 kPa). The as-received media appeared to retain much of the dust cake that was present during bag removal. The average as-received Frazier number was 2.42 after 8 weeks (1360 hr) of operation at a 12 ft/min (3.66 m/min) A/C ratio. After brushing, the average Frazier number was 6.57 after 8 weeks. The after-brushing Frazier number is within the range of the new media permeability. This indicates the membrane is capturing the particles on the surface of the media while retaining most of its original permeability.

The air permeability analysis of the AHPC Filter Bag (R4B7) after 670 hr of operation was performed in the lab using the Frazierometer. The identical procedure for the time period of April to June was followed (see Table 3). The average as-received Frazier number for R4B7 was 2.22 and after brushing was 5.44.

TABLE 3

Filter Media Permeability as Measured in Lab

Time Period Bags in Operation	Hours of Operation	Bag Position	As-Received Average of Nine Data Points, ft/min at 0.5 in. W.C.	After-Brushing Average of Nine Data Points, ft/min at 0.5 in. W.C.
April 18 to June 26	1360	R3B3	2.48	5.82
April 18 to June 26	1360	R3B6	2.86	5.91
April 18 to June 26	1360	R4B4	1.77	4.37
April 18 to June 26	1360	R4B7	1.53	5.61
April 18 to June 26	1360	R2B1	2.33	4.78
April 18 to June 26	1360	R1B5	2.82	5.92
April 18 to June 26	1360	R2B2	3.17	7
		ave.	**2.42**	**6.57**
June 26 to July 21	670	R4B7	2.22	5.44

5.5 Mechanical Strength Analysis

A Mullen Burst test was run on Filter Bag R4B7 after 670 hr of operation. The sample was removed from the center of the filter bag to determine if any weakening of the bag had occurred. The test gradually applies increasing pressure behind the filter bag sample until the test unit's rubber diaphragm penetrates the sample. The sample burst at 1000 psi (6895 kPa), indicating no chemical or thermal attack had occurred. The Mullen Burst strength for a new bag typically falls in the range of 500 to 1000 psi (3447 to 6895 kPa).

5.6 Summary of Bag Evaluation

- The filter bags retained permeability and recovered from system upsets, including switches to different coal sources.

- A new start-up procedure due to switching coal sources will be followed and include precoating the bags during start-up.

- The damage to the membrane is due to electrical effects on the bags. The new components and spacing may have contributed to these effects.

6.0 COLD-FLOW TESTS AT THE EERC

To evaluate the cause of the bag damage observed in the Big Stone field study, experiments were carried out at an EERC laboratory to investigate the interactions between electrostatics and

bags under different operating conditions. The 200-acfm (5.7-m^3/min) AHPC was operated without fly ash under cold-flow conditions with air.

The experimented parameters are summarized below:

Electrode type: EERC, EX, EN 3-mast, EN 2-mast, Pipe

Bag type: GORE-TEX® membrane/GORE-TEX® felt filter bags (NBNM)
GORE-TEX® conductive membrane/GORE-TEX® felt filter bags (NBCM)
GORE-TEX®-NO STAT® filter bags (CBNM)
GORE-TEX®-NO STAT® filter bags with GORE-TEX® conductive membrane (CBCM)
SUPERFLEX® filter bags
RYTON® felt (no membrane)

Plate spacing: 600 mm, 700 mm, 800 mm

Spacing ratio: 1.00, 1.25, 1.65, 2.00

Grounded grid: 2-wire grid, 3-wire grid, diamond mesh

A total of five different electrodes were used in the cold-flow test to examine their effects on current to the bags. Detailed information about these electrodes is listed in Table 4.

TABLE 4

Electrode Type and Discharge Points

Electrode Type	Spacing Between Electrode Masts, cm	Electrodes Used per Side	Discharge Points per Electrode	Total Discharge Points
EERC	10	7	34	476
EX	38	2	16	64
EN 3-Mast	19	2	22	88
EN 2-Mast	38	3	22	132
Pipe	19	3	0	0

A number called the “spacing ratio” was created to compare the distances and position of the discharge electrode relative to the filter bag and collecting plate. The ratio is equal to the distance of the bag-to-electrode divided by the distance of the electrode-to-plate.

In order to suppress the back corona observed on the bag surface, metal-grounded grids were installed between the bags and electrodes. Three different types of grounded grids, called 2-wire, 3-wire, and diamond mesh, were tested. The 2-wire grid consisted of two vertical wires,

3 mm in diameter, spaced 60 mm apart in front of each filter bag. The total number of wires per bag side was eight. These were placed 25 mm from the bag surface. The 3-wire was similar, except with three wires in front of each bag. The diamond mesh was a diamond pattern plate grid of expanded metal with a diamond hole size of 20 mm × 30 mm. Each plate was positioned 30 mm from the bag's surface between the bags and the discharge electrodes.

The response variables were the measurement of the electrical current flow through the bags, cages, and the collecting plates and observations of back corona. The cages, bags, and collecting plates were isolated from grounded points. Each cage and plate had an independent ground wire.

A negative-polarity HV was applied to the discharge electrodes. The ground wires connected to each filter cage and collecting plate traveled through independent current meters to an earth ground. Six current readings were taken simultaneously: four from the bags and two from the collecting plates. All the measurements were totaled and compared to the current output by the HV power supply. Calculating the sum of the total bag current and the plate current as a percentage of the total current produced by the power supply yielded percentages of 92%–100% without a grounded grid. Replicate tests were completed showing very accurate and repeatable results.

The power supply is capable of producing 10 mA at up to 100 kV. Typically, the 10 mA current limit was reached between 60 and 75 kV. The direction of current flow in the ammeter was always in the same direction, starting from 0 amps at 15 kV and up to 1 mA through a filter bag and cage. The current meter always displayed a negative value and did not switch polarity when back corona was observed.

Observations of the corona discharge from the electrodes and bags were made through site ports of the AHPC pilot unit. All other entry points of light were eliminated so that total darkness was produced inside the AHPC chamber. After one's eyes adjusted to the darkness, observations of corona and back corona were noted.

6.1 Effect of Electrodes on V-I Characteristics and Current to Bags

A series of experiments was first carried out to investigate the effectiveness of different type electrodes on the corona current. Plate spacing was set to 600 mm, and GORE-TEX® conductive felt with nonconductive membrane bags (CBNM) was used. A total of five electrode types were tested under two different spacing ratios of 1.25 and 1.65. The total generated corona currents were plotted as a function of applied voltage, shown in Figures 17 and 18. Under the two spacing ratios of 1.25 and 1.65, the EERC electrode produced the highest total corona current followed by EX, EN-3, and EN-2 type electrodes. The pipe electrodes produced a much lower corona current. The current to bags was also measured simultaneously at the two ratios as shown in Figures 19 and 20. The EX electrode induced up to 48% of the total generated corona current to the filter bags. EN-3 type electrodes generated almost the same total current as that of EX under similar operating conditions, but only around 22% of the total corona current reached the bags. The pipe electrodes had less than 0.5 mA current to bags at an applied voltage of 60 kV,

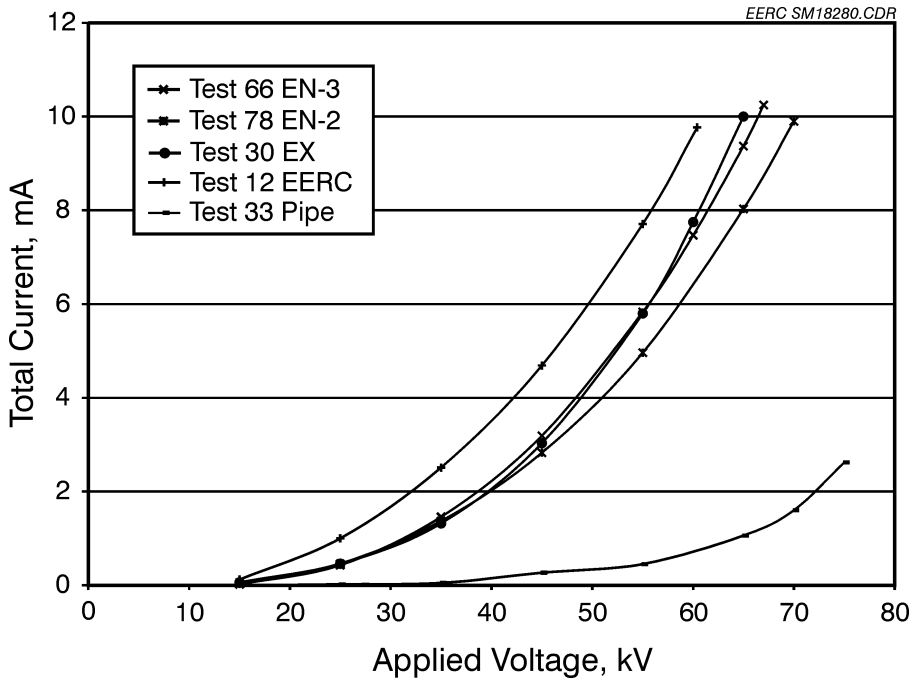

Figure 17. Effect of electrode on V-I characteristics (ratio – 1.25, plate spacing – 600 mm, bags – CBNM).

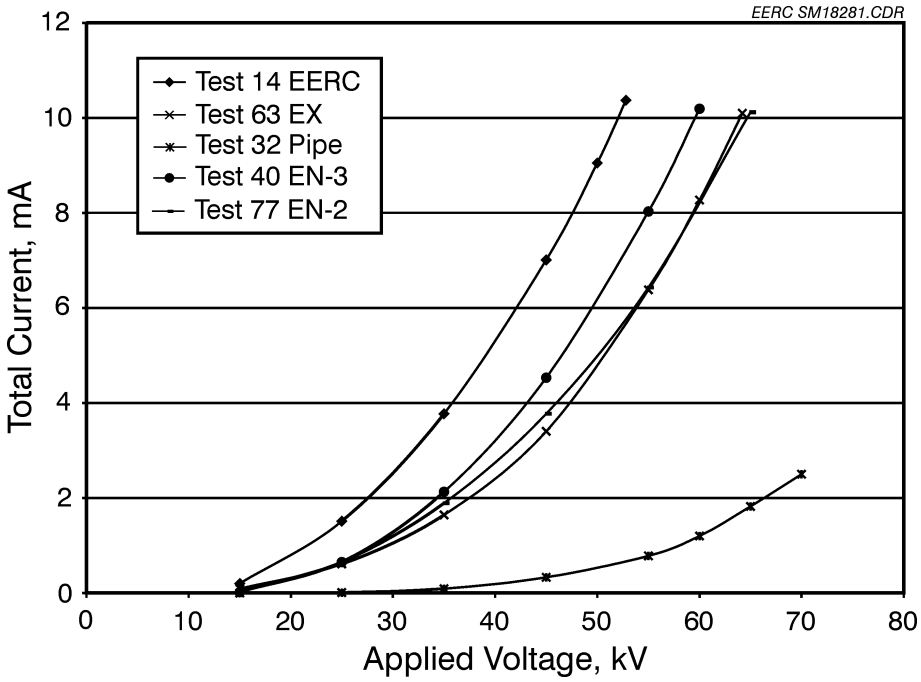

Figure 18. Effect of electrode on V-I characteristics (ratio – 1.65, plate spacing – 600 mm, bags – CBNM).

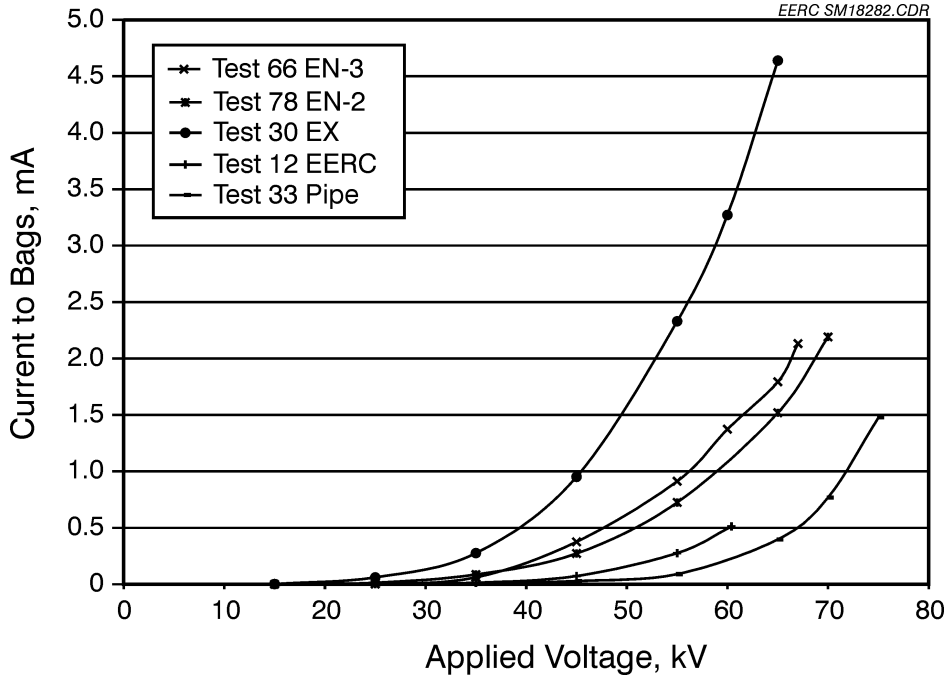

Figure 19. Effect of electrode on current to bags (ratio – 1.25, plate spacing – 600 mm, bags – CBNM).

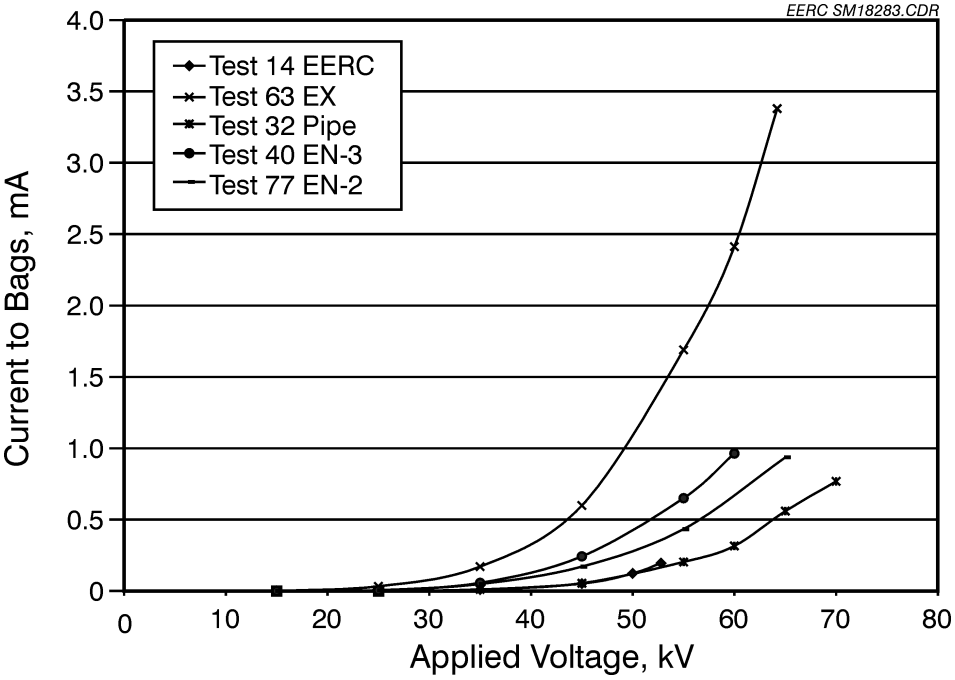

Figure 20. Effect of electrode on current to bags (ratio – 1.65, plate spacing – 600 mm, bags – CBNM).

but this was more than 50% of the total corona current. The EERC electrode demonstrated a low current to bags of 0.5 mA at an applied voltage of 60 kV, which was only 5.0% of the total corona current.

These experimental results indicated the EERC electrode was the best in terms of higher total corona current and lower current to bags, followed by the EN-type electrodes which also had satisfactory results. The EX electrodes had a high total corona current generated, but a large portion of the current went to bags, which is likely to produce back corona on the bag surface. The pipe electrodes minimize current to the bags, but the total current is too low to be used in the AHPC.

6.2 EERC Electrode Tests

Experiments were conducted to examine the effects of bag type, plate spacing, and spacing ratio on the current to the bags with different types of electrodes. The effectiveness of metal-grounded grids on suppression of back corona was also investigated.

The total current to the bags was measured as a function of applied voltage under spacing ratios ranging from 1.00 to 2.00. The higher the spacing ratio, the closer the electrodes were to the collection plates compared to the distance from the electrodes to the bags. The results, shown in Figure 21, indicate the current to the bags decreases with increasing spacing ratio. The total current to the bags nearly dropped to zero when the spacing ratio was 2.00. However, part of the electric precipitation zone was sacrificed to achieve a lower current level to the bags. Experimental data demonstrated a wider plate spacing (from 800 to 600 mm) resulted in a decrease of current to the bags, as shown in Figure 22. Even though a higher total current was recorded at an applied voltage of 65 kV with plate spacing of 600 mm compared to that of 800 mm, the percentage of current to bag was 14.9% for the plate spacing of 800 mm compared to 17.4% for the plate spacing of 600 mm. The presence of the 2-wire grounded grid reduced the current to the bags at a spacing ratio of 1.00 (shown in Figure 23).

6.3 EX Electrode Tests

The total current to the bags was measured as a function of applied voltage under spacing ratios ranging from 1.25 to 2.00 at a plate-to-plate spacing of 600 mm, as shown in Figure 24. The higher spacing ratio resulted in a decrease of current to the bags; however, with the EX electrode, there was still significant current to the bags even at the ratio of 2.00. The back corona on the bags was very bright at the ratio of 1.25 and became faint at the ratio of 2.00.

In addition to the corona emitting from the electrode tips pointed toward the plates, corona in some locations was also seen to point away from the plates and toward the filter bags. Back corona off the bags was observed to be much brighter in locations opposite these corona discharge points. This suggests that the EX electrode is not highly directional and explains why much higher bag currents were seen with this design. It also suggests that the lack of directional specificity is a likely cause of the bag damage seen in the field tests (the EX electrodes are the type installed in the 9000-acfm (255 m^3/min) AHPC at Big Stone).

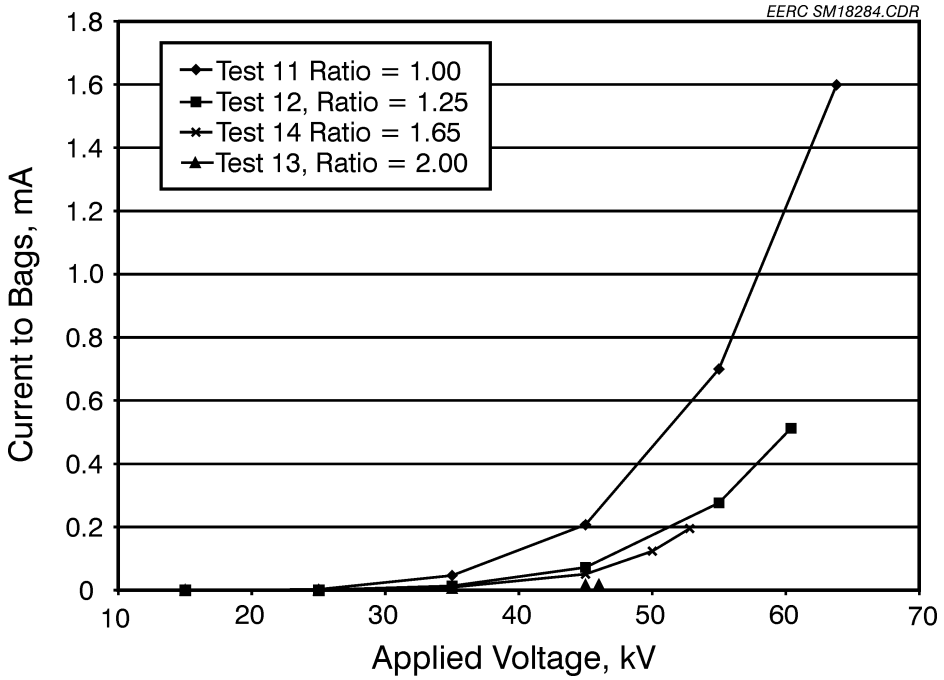

Figure 21. Effect of spacing ratio on bag current (EERC electrode, bags – CBNM, plate spacing – 600 mm).

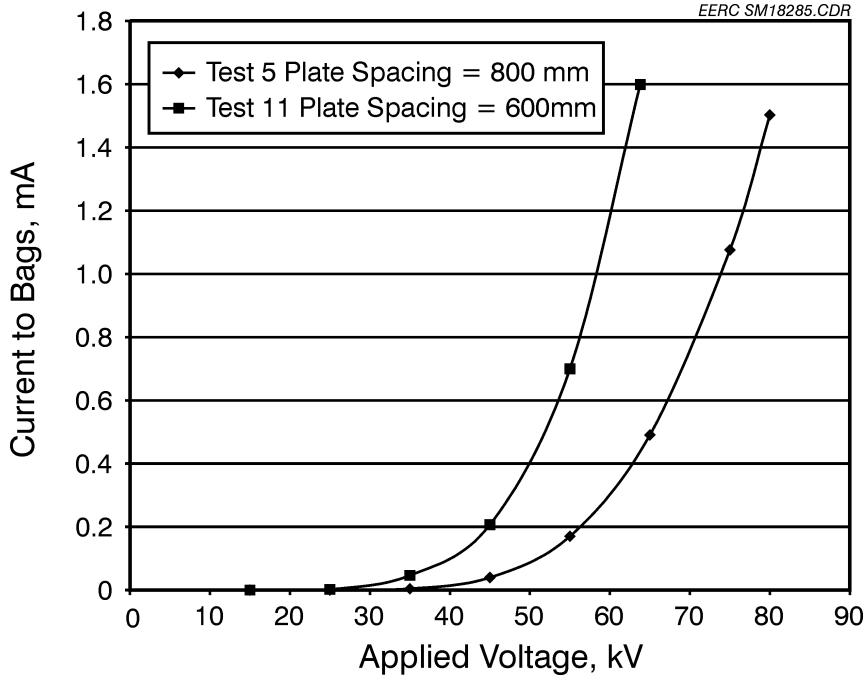

Figure 22. Effect of plate spacing on bag current (EERC electrode, ratio – 1.00).

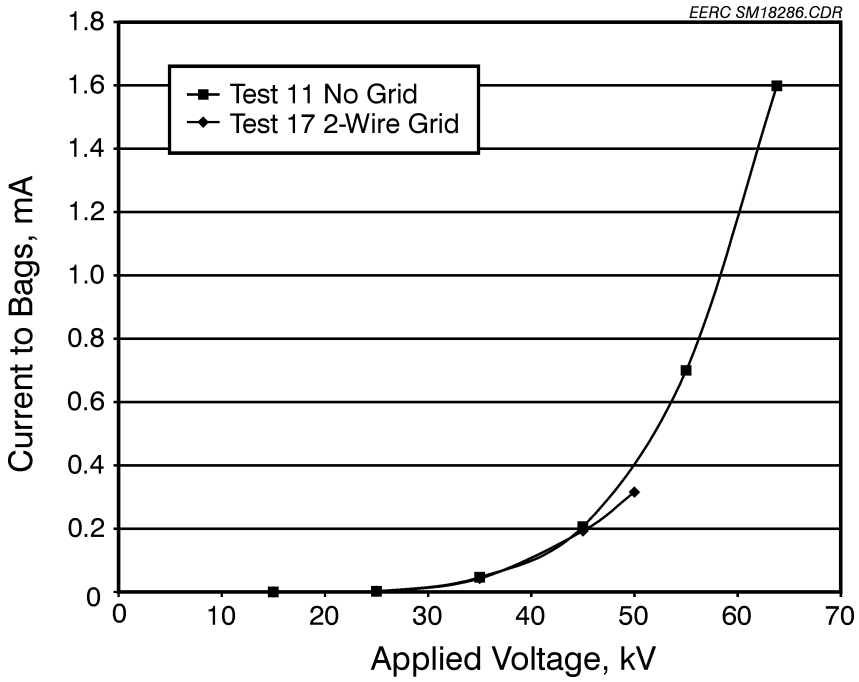

Figure 23. Effect of grid on bag current (EERC electrode, ratio – 1.00, plate spacing – 600 mm).

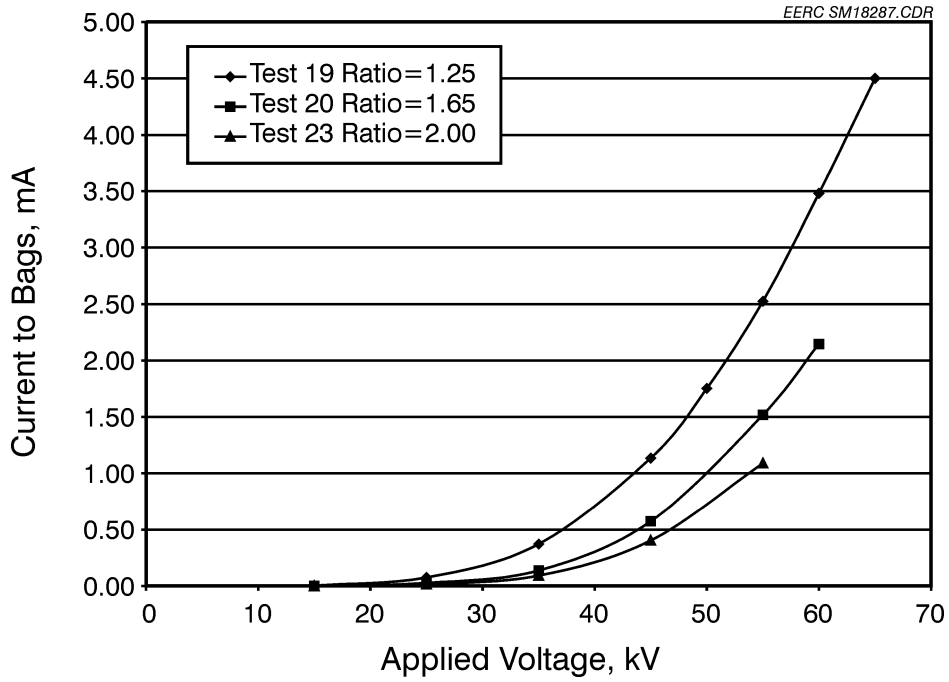

Figure 24. Effect of ratio on current to the bags (EX electrode, bags – CBNM, plate spacing – 600 mm).

The effect of bag type on the current to the bags under a plate-to-plate spacing of 600 mm and two different ratios of 1.25 and 2.00 is shown in Figures 25 and 26. The conductive felt and conductive membrane bags (CBCM) demonstrated the best performance in terms of the minium current to the bags compared to the other type bags. However, there was significant current to the bags for all of the bag types for both ratios. Therefore, a change in bag type alone is not likely to sufficiently lower the bag current for the EX electrode.

In order to further reduce the current to bags, grounded grids were designed and installed between the bags and the electrodes. Results (Figure 27) show that the current to the bags was significantly reduced from 1.1 mA at an applied voltage of 55 kV to 0.42 mA in the presence of the 2-wire grounded grid and nearly dropped to zero by using the diamond mesh grounded grid. These results indicate that bag current can be significantly reduced by installing an appropriately designed grounded grid between the discharge electrodes and the bags.

6.4 EN Electrode Tests

The total current to the bags was measured as a function of applied voltage under spacing ratios ranging from 1.25 to 2.00, and the results are shown in Figure 28. The bags used were GORE-TEX® conductive felt and conductive membrane (CBCM), while the GORE-TEX® conductive felt with nonconductive membrane (CBNM) bags were used in the EERC and EX electrode tests. The higher spacing ratio resulted in a decrease of current to bags, similar to that observed for the other electrodes. The current to the bags was more than 2 mA at the ratio of 1.25 under the applied voltage of 60 kV. With the spacing ratio adjusted to 1.65, the total current to the bags was significantly reduced to 0.5 mA at the applied voltage of 60 kV. The same trend of decreasing current to the bags at a higher spacing ratio was also seen at a wider plate spacing of 700 mm with CBNM bags, as shown in Figure 29. Some back corona was also observed on the filter bags at all of the ratios tested.

Experiments were then performed to investigate the current to the bags as a function of bag type at a plate-to-plate spacing of 600 mm and a spacing ratio of 1.25. The experimental data (Figure 30) show more current was attracted to the bags with the CBNM bags compared to the CBCM bags, similar to the results with the EX electrode. For comparison, the current with cages only (no bags) is shown to be much less than the current with bags.

The effectiveness of a grounded grid on the reduction of current to bags was examined by using the 3-wire grounded grid with different type bags. The experimental data, shown in Figure 31, demonstrated a significant reduction of the current to the bags compared to that plotted in Figure 30. Again, the CBNM bags had the highest current to the bags of 0.17 mA at the applied voltage of 67 kV. However without the grounded grid, the current was 2.2 mA at 67 kV, so the grid reduced the current to the bags by over 90%.

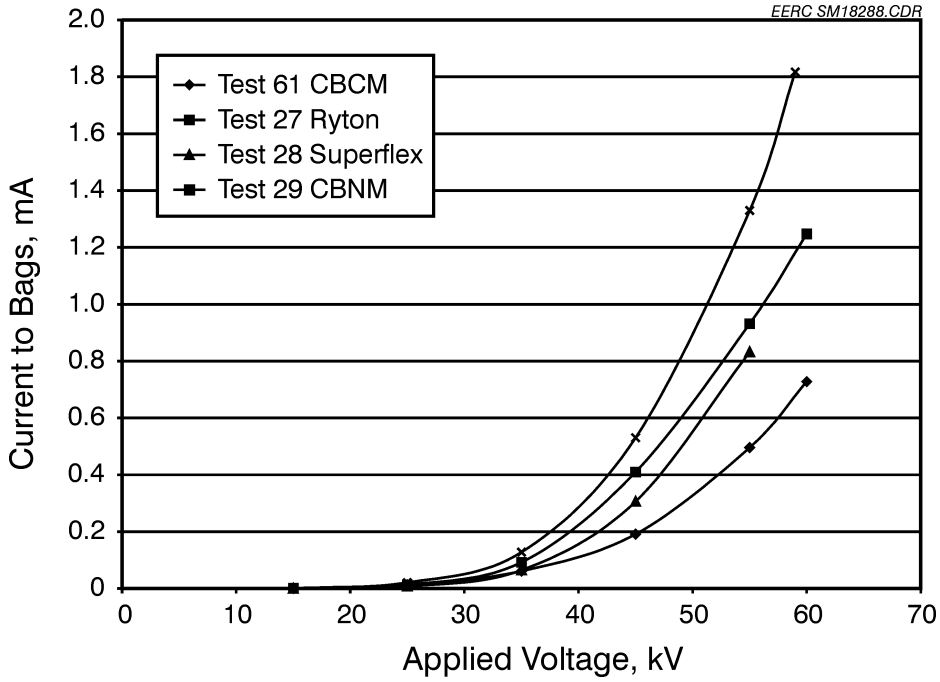

Figure 25. Effect of bag type on current to the bags (EX electrode, plate spacing – 600 mm, ratio – 2.00).

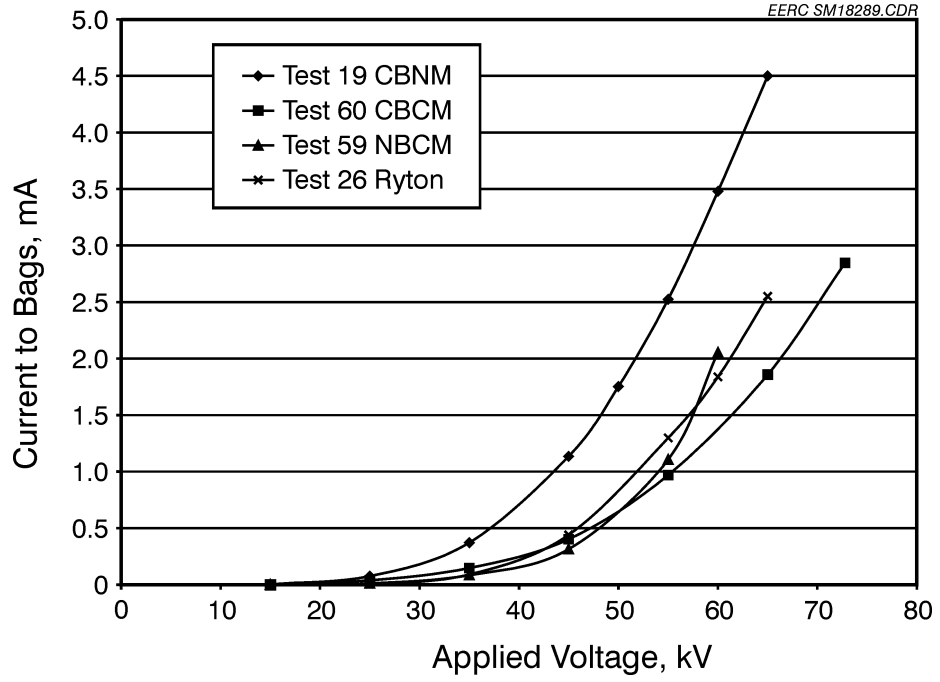

Figure 26. Effect of bag type on current to the bags (EX electrode, plate spacing – 600 mm, ratio – 1.25).

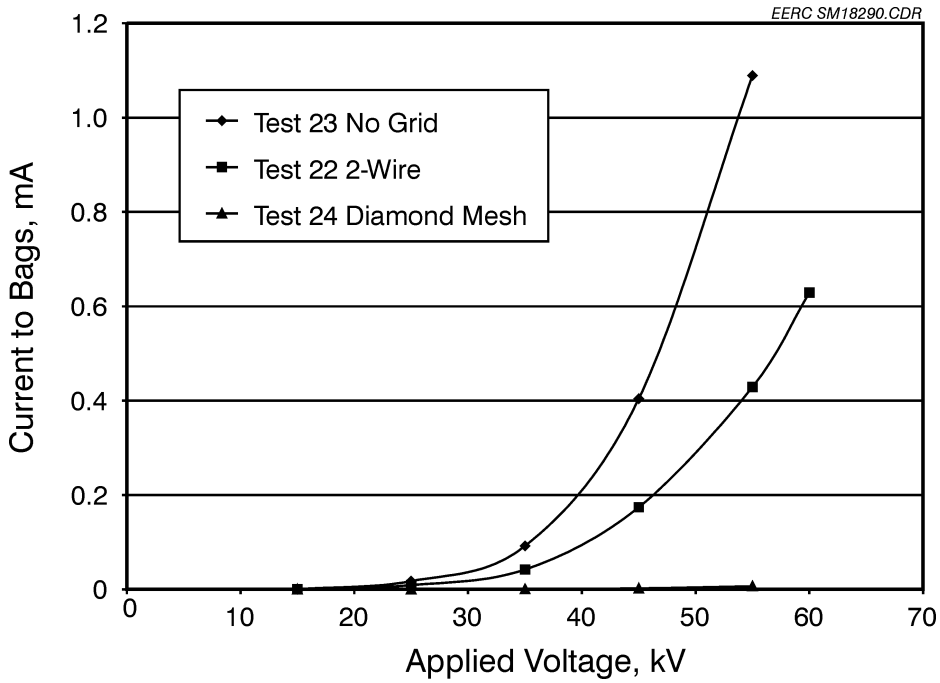

Figure 27. Effect of grounded grid on current to the bags (EX electrode, plate spacing – 600 mm, ratio – 2.00).

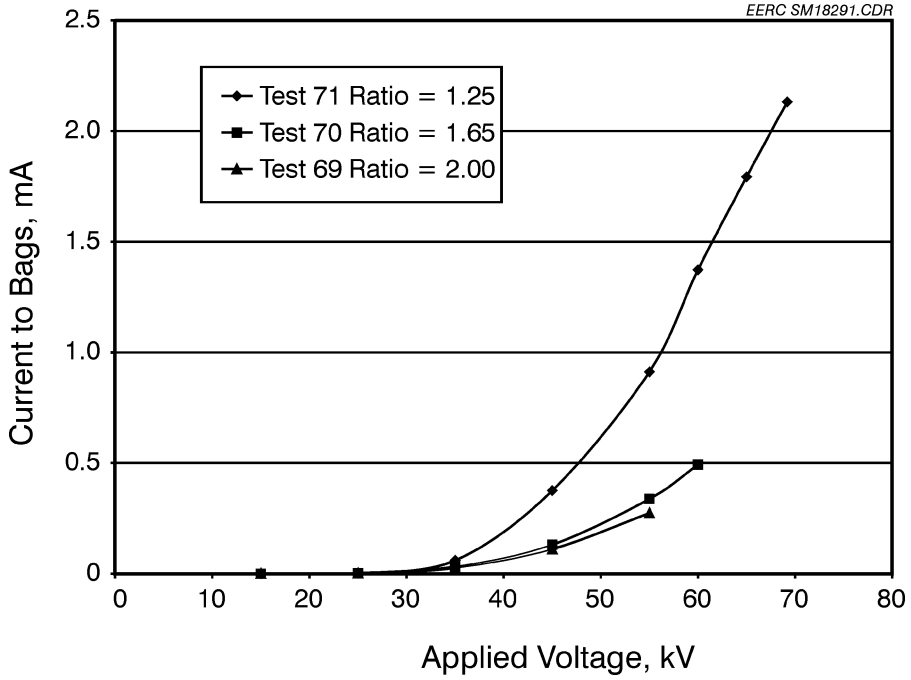

Figure 28. Effect of ratio on current to the bags (EN-3 electrode, plate spacing – 600 mm, bags – CBCM).

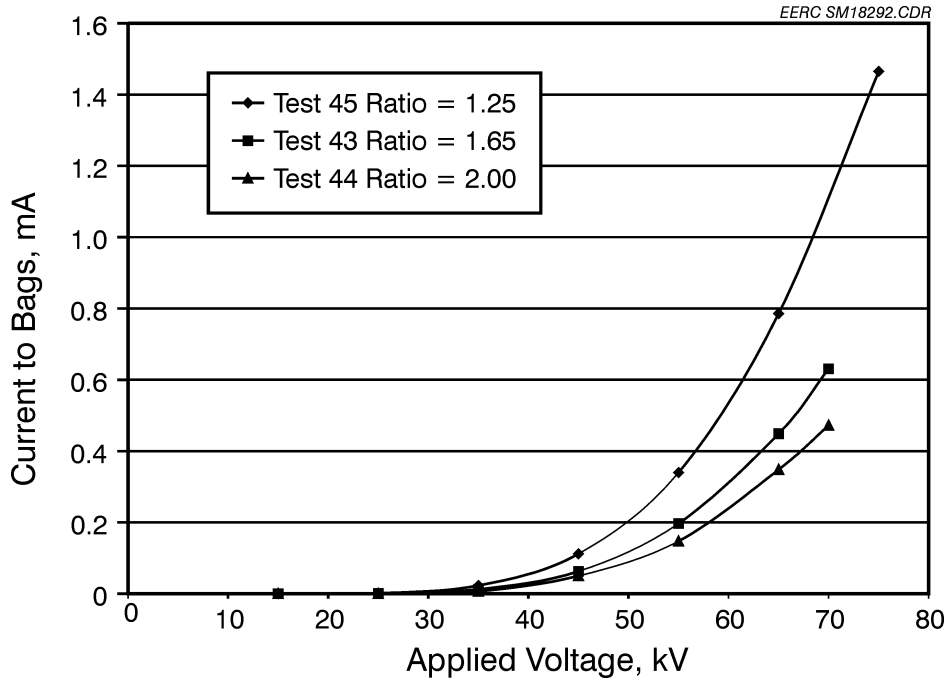

Figure 29. Effect of ratio on current to the bags (EN-3 electrode, plate spacing – 700 mm, bags – CBNM).

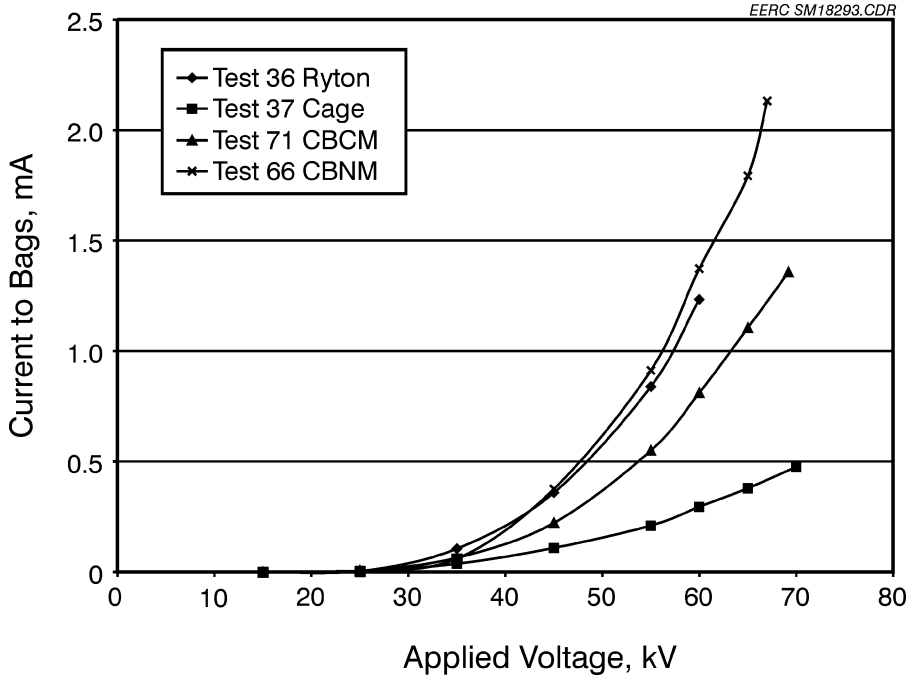

Figure 30. Effect of bag type on current to the bags (EN-3 electrode, plate spacing – 600 mm, ratio – 1.25).

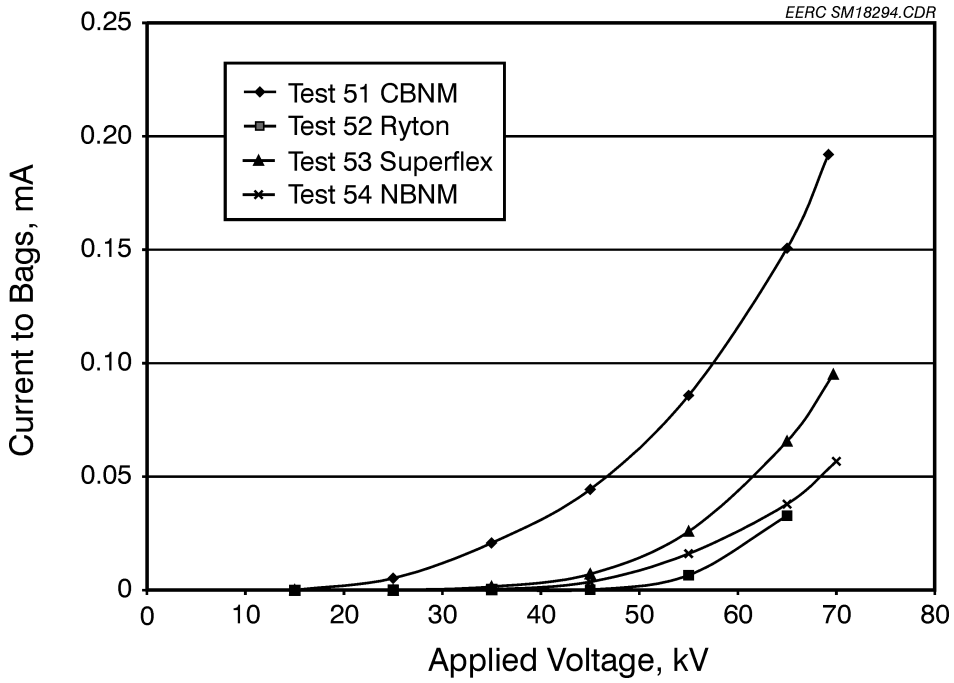

Figure 31. Effect of bag type on current to the bags in the presence of a grounded grid (EN-3 electrode, plate spacing – 600, ratio – 1.25, 3-wire grid).

6.5 Summary of the Cold-Flow Tests

- Electrode type, bag type, spacing ratio, plate-to-plate spacing, and grounded grids were all evaluated for their effect on the current to the bags in cold-flow tests without dust. The most significant factors were electrode type, spacing ratio, and the presence of a grounded grid.

- A significant finding was that the EX-type electrode, which is the type installed on the Big Stone AHPC had the highest current to the bags and appeared to be less directional than either the EERC or EN types. By switching from the EX electrode to another type, it is likely that the current to the bags can be significantly reduced.

- Spacing ratio was also a major factor affecting the amount of current to the bags. The spacing ratio tests indicate that the amount of current to the bags can be significantly reduced by increasing the ratio.

- The grounded-grid tests show that a simple wire grid can greatly reduce the current to the bags, but that a more dense arrangement such as a diamond pattern-expanded metal grid can reduce the current to almost zero.

- The plate-to-plate spacing tests showed that, at the same spacing ratio, a wider plate-to-plate spacing will also reduce the current to the bags.

- The CBCM bags had a lower bag current than the CBNM bags. Since the CBNM bags were the type previously used at Big Stone, an approach to reduce the amount of current to the bags is to replace them with the CBCM type.

While the tests show clear effects of these variables on the level of current to the bags, the results need to be verified in further cold-flow testing with dust and then under real flue gas conditions.

7.0 PLANS FOR NEXT QUARTER

During the next quarter (October–December), additional pilot-scale testing with the 200-acfm (5.7 m^3/min) AHPC will be conducted to further evaluate the best electrode and spacing arrangement to be implemented on the 9000-acfm (255 m^3/min) AHPC nat Big Stone. It is anticipated that any changes to the 9000-acfm (255 m^3/min) AHPC will also be started during the next quarter.